

Spectral statistics of nondiffusive disordered electron systems: A comprehensive approach

Alexander Altland* and Yuval Gefen

Department of Condensed Matter Physics, The Weizmann Institute of Science, 76100 Rehovot, Israel

(Received 8 December 1993)

We present an analysis of the two-level correlation function (K) and the fluctuation of the level number (Σ_2) within an energy interval E of disordered conductors. Our analysis extends to nondiffusive regimes, including E larger than the inverse elastic scattering time \hbar/τ and ballistic (but not perfectly clean) systems. Technically, our perturbational approach goes beyond the common diffusion and cooperon approximation. We find additional types of behavior for K and Σ_2 . These manifest in the large-energy ($E > \hbar/\tau$) nonuniversal regime, which is studied vis-à-vis general features of the scattering potential. The impurity-averaged correlation function is contrasted with energy-averaged correlators often employed in the context of quantum chaos. Various composite correlation functions, defined with respect to energy, disorder, and possibly sample-size-averaging procedures, are introduced and calculated. This provides a bridge between the physics of clean chaotic and disordered systems. We extend our analysis to the case of an external magnetic field that is applied to a diffusive sample. We address the question of how strong magnetic fields, corresponding to magnetic lengths smaller than the elastic mean free path, affect the spectral statistics.

I. INTRODUCTION

Mesoscopic systems exhibit plenty of fingerprint-type phenomena, i.e., the measured values of *macroscopic* observables often depend sensitively on the *microscopic* parameters characterizing the system at hand. Two macroscopically identical mesoscopic systems, for example, may yield very different results for magnetization and conductance as functions of an external magnetic field. Similar sensitivity to system parameters typifies chaotic systems. The study of systems exhibiting fingerprint phenomena can often be reduced to the analysis of the corresponding quantum-mechanical energy spectra. A few examples in this context are as follows: The averaged magnetization of an array of quantum dots (within the canonical ensemble) is related to the fluctuations of the level number over a field-dependent energy scale.¹⁻³ The phenomenon of persistent currents in small normal conductor rings is closely connected with level correlations at the Fermi energy.⁴⁻⁶ The ac conductivity of an isolated mesoscopic conductor $\sigma(\omega)$ is connected with correlations over an energy scale ω .⁷ Other fluctuation phenomena (including conductance and magnetic-susceptibility fluctuations) are connected with spectral correlations, as well. An exhaustive statistical description of random energy spectra is a highly complicated, and in many cases, an unmanageable task. Many mesoscopic phenomena, however, including those itemized above, can be discussed by relating them to the most elementary correlation function characterizing a stochastic spectrum. This function, which is often denoted by K , will be defined below.

Besides its importance for practical applications, the correlation function K also plays a more fundamental role as a source of information about the charge carrier *dynamics*: Within the semiclassical approximation (cf.,

e.g., Ref. 8), the energy Fourier transform of K represents a measure for the classical probability for electron motion along periodic orbits (a more precise formulation of this statement will be given below). So far, the correspondence between classical dynamics on the one hand and spectral correlations induced by the presence of disorder on the other hand has only been elaborated in cases where the dynamics is governed by diffusive motion. On the other hand, the derivation presented in Ref. 8, as it relies only on the applicability of the semiclassical approximation,⁹ should extend throughout a much wider domain including, in particular, the nondiffusive regimes treated in this paper. Indeed, it will turn out that many of the results derived below (in a fully quantum-mechanical formulation) can be given a vivid *a posteriori* interpretation by relating them to the classical dynamics of electrons in the regime under consideration.

Spectral correlations are of fundamental importance in the context of quantum chaos as well. One is typically interested in the behavior of quantum particles moving *freely* within certain geometries. Such systems will be referred to as *clean* systems. Depending on a clean system's geometry, the corresponding dynamics may be governed by chaotic or regular motion. Besides the confining geometry, microscopic disorder may render the motion of quantum particles chaotic as well. This explains the far reaching analogies between the physics of clean chaotic and disordered mesoscopic systems, respectively. To classify these analogies, it is convenient to distinguish between at least four different ranges of disorder strength. As a preliminary stage to the definition of the various disorder regimes, we list the relevant length and energy scales. Throughout this paper an $\hbar=c=1$ convention will be employed.

The *length scales* are as follows.

L is the linear size of the system.

l_ϕ is the phase-breaking length, i.e., the scale beyond

which a single electron may not be described by a coherent quantum-mechanical wave function. Dephasing may be caused by electron-electron collisions, by the interaction of the electron with external degrees of freedom, or by temperature-induced energy averaging.

ξ is the Anderson localization length (localization always occurs in systems of dimensionality $d \leq 2$ or, otherwise, for sufficiently strong disorder).

l is the elastic mean free path. For soft scattering potentials one has to distinguish between the mean free path between subsequent scattering events, and the (longer) scale characterizing the randomization of the particle's original momentum, the latter scale is of relevance for transport coefficients.

λ_F is the Fermi wavelength (the inverse Fermi momentum $\lambda_F \equiv 2\pi p_F^{-1}$). Unless we are in the strong disorder limit the inequality $p_F l \gg 1$ holds.

The relevant *energy scales* are as follows.

E_F is the Fermi energy.

τ^{-1} is the inverse elastic mean free time. Similarly to our preceding remarks one may distinguish between the elastic-scattering time and the transport mean free time (associated with large momentum transfer).

t_f^{-1} is the inverse time of flight of electrons at the Fermi energy through a ballistic system $t_f^{-1} \equiv v_F L^{-1}$. Here v_F is the Fermi velocity.

E_c is the Thouless (or correlation) energy $E_c = DL^{-2}$, equal to the inverse diffusion time through a diffusive system.

τ_ϕ^{-1} is the inverse dephasing time.

Δ is the mean level spacing at the Fermi energy.

We next review the classification of disordered mesoscopic systems ($L < l_\phi$) according to the degree of disorder. The scheme applies to systems of integrable geometry.

For *strongly localized systems*, $L \gg \xi$.

For *diffusive systems*, $l \ll L \ll \xi$, or in terms of energy parameters $\Delta \ll E_c \ll \tau^{-1} \ll E_F$.

For *ballistic systems*, $lM^{-1} \ll L \ll l$ or $\Delta \ll \tau^{-1} \ll t_f^{-1} \ll E_F$. Here M is the number of transverse channels. The inequality involving length scales may also be written as $1 \ll lL^{-1} \ll (p_F L)^{d-1}$.

For *perturbative (nearly clean) systems*, $lL^{-1} \gg (p_F L)^{d-1}$ or $\Delta \gg \tau^{-1}$. These conditions imply that the typical matrix element of the scattering potential is smaller than the level spacing. It follows that the spectrum may be obtained from the underlying clean spectrum employing low-order perturbation theory. Note the distinction between nearly clean and ballistic systems, the former imposing more severe conditions on the system size.

In the present work we consider an electron confined to move in a regular geometry—in our case a two-dimensional square.¹⁰ In the absence of intrinsic scattering the motion of a classical particle in such a potential is integrable. In general the corresponding single-particle energy spectrum obeys (nearly¹¹) Poissonian statistics (degeneracies caused by symmetries, as they occur, e.g., in square geometries, may cause deviations from this behavior). The introduction of impurities or imperfec-

tions renders the motion of the electrons chaotic. Thinking in terms of semiclassical trajectories, one should not expect qualitative differences between the motion of particles in disordered and chaotic systems on sufficiently large time scales. Evidently, the degree of disorder will dictate the relevant time scales needed to observe chaoticity. In a more quantum-mechanical picture the disorder gives rise to a mixing of the clean system's energy levels, thereby inducing spectral *correlations*. The extent of correlation between energy levels depends predominantly on the disorder strength (measured by τ^{-1}) and their distance E . As has been verified for diffusive systems and energies $E < \tau^{-1}$, there exist various qualitatively different regimes of correlations. It has been speculated that fluctuations in the level number obtained within an energy window ΔE saturate as ΔE exceeds $1/\tau$.

Surprisingly enough, this question, although having important bearing on the physics near the Fermi energy, has not been settled until recently. Even more importantly, it has not been realized that ballistic (according to the definition above) systems may exhibit interesting types of behavior that are profoundly distinct from the physics of clean systems, contrary to some misleading statements in the literature. As has been pointed out in Ref. 12, significant mixing of the clean system's levels and nontrivial spectral correlations may be encountered even under the condition $L < l$. Evidently these extensions of the analysis of spectral correlations to nondiffusive regimes bear consequences on the effects of magnetic fields too. One may study the effect of weak fields in regimes which are nondiffusive even in the field-free case. Alternately one may investigate the influence on strong fields (in a sense that will be defined below) on diffusive systems. All cases have in common that the prerequisite of a generally diffusive dynamics is to be abandoned.

The first major goal of the present paper is to extend the study of spectral correlations beyond the diffusive regime. To this end we develop a perturbative technique that is more general than the standard approach in so far as it does not invoke the standard diffusion and cooperon approximation. Within that formulation we analyze the nondiffusive regimes and recover some known results in order to relate our approach to earlier works. Exploiting the above-mentioned connection between spectral correlations and classical dynamics, we relate our results to the dynamical behavior of charge carriers in the nondiffusive regimes. The second goal of this paper is to compare the *disorder-averaged* two-level correlation function with the *energy-averaged* correlation function commonly employed in the field of quantum chaos. We discuss qualitative differences between both quantities and propose a generalization of the latter to include the presence of impurity scattering. We believe that this constitutes another step in bridging the two disciplines of mesoscopic physics and quantum chaos.

The outline of this paper is as follows: In Sec. II we define our model system and outline the perturbative approach used to calculate the correlation function K . Results for the field-free case, both for diffusive and ballistic systems are presented. Nonuniversal features of the

correlations and the smooth scattering potentials are discussed in Sec. III. In Sec. IV we generalize the definition of the two-level correlation function to include energy averaging and relate it to the correlation functions commonly used in the context of quantum chaos. Magnetic fields are discussed in Sec. V and a few concluding remarks are presented in Sec. VI. Technical details of our analysis are provided in the appendixes.

II. CALCULATION OF THE TWO-LEVEL CORRELATION FUNCTION

We now turn to the concrete calculation of the two-level correlation function. Let us represent our model system of noninteracting electrons moving in a disordered potential and a magnetic field by the Hamiltonian

$$\mathcal{H} = H_0 + V,$$

where in a self-evident notation

$$H_0 = \frac{1}{2m}(p - eA)^2$$

and V is a white-noise potential defined by the correlator

$$\begin{aligned} \langle V(x) \rangle &= 0, \\ \langle V(x)V(y) \rangle &= \frac{1}{2\pi\nu\tau} \delta(x-y). \end{aligned} \quad (1)$$

Here, τ is the scattering time (of electrons moving at the Fermi surface), $\nu = \nu(E_F)$ the density of states per unit volume at the Fermi energy E_F , and the angular brackets denote the disorder average. At present we specify neither the system geometry nor the magnetic field. The generalization of Eq. (1) to different types of disorder potentials will be discussed in a subsequent section.

Our aim is to calculate the two-level spectral correlation function

$$\begin{aligned} K(\epsilon_1, H_1; \epsilon_2, H_2) &= \frac{1}{\nu^2} [\langle \nu(\epsilon_1, H_1) \nu(\epsilon_2, H_2) \rangle \\ &\quad - \langle \nu(\epsilon_1, H_1) \rangle \langle \nu(\epsilon_2, H_2) \rangle], \end{aligned} \quad (2)$$

describing the *disorder-induced* correlation between two energy levels ϵ_1 and ϵ_2 (and the magnetic fields H_1 and H_2) close to the Fermi energy and the related quantity

$$\begin{aligned} \Sigma_2(E, H_1, H_2) &= \Delta^{-2} \int_{E_0 - E/2}^{E_0 + E/2} d\epsilon_1 d\epsilon_2 K(\epsilon_1, H_1; \epsilon_2, H_2), \\ E_0 &= O(E_F), \end{aligned} \quad (3)$$

which measures the level number fluctuations in an energy strip of width ΔE . Note that both quantities, contrary to the energy-averaged correlation functions commonly employed in the context of quantum chaos, vanish in the limit of no disorder and should be carefully distinguished from the latter. As will become evident below, K depends only on the difference $\omega \equiv \epsilon_1 - \epsilon_2$ between the levels, except for corrections in the small parameter $(\epsilon_1 - \epsilon_2)E_F^{-1} \ll 1$. Similarly, Σ_2 is independent of the center coordinate E_0 . Expressed in terms of single-electron Green functions,

$$\mathcal{G}^\pm(\epsilon, H) = (\epsilon^\pm - \mathcal{H})^{-1}, \quad \epsilon^\pm = \epsilon \pm i\delta, \quad (4)$$

the correlation function takes the form

$$\begin{aligned} K(\epsilon_1, H_1; \epsilon_2, H_2) &= \frac{\Delta^2}{\pi^2} \langle \text{tr} \text{Im} \mathcal{G}^+(\epsilon_1, H_1) \text{tr} \text{Im} \mathcal{G}^+(\epsilon_2, H_2) \rangle_c, \end{aligned} \quad (5)$$

where the subscript c indicates the omission of all disconnected contributions to the average and where Δ denotes the mean level spacing at the Fermi surface. In order to evaluate this expression to leading order in the disorder parameter $p_F l \gg 1$, we employ the methods of diagrammatic perturbation theory. The applicability of perturbation theory is restricted to energy differences ω , which are large in comparison with the mean level spacing Δ . For energy differences smaller than Δ , the diagrammatically evaluated result exhibits an unphysical divergence and nonperturbative techniques have to be applied. The emergence of this divergence can be avoided by smearing the individual energy levels according to $\epsilon^\pm \rightarrow \epsilon^\pm + i\gamma$, $\gamma = O(\Delta)$.¹³ For the sake of notational simplicity, we denote the smeared levels again by ϵ^\pm . On energy scales larger than Δ , this manipulation does not affect the spectral properties of the model and it permits one to apply perturbation theory throughout the entire spectrum.

In order to evaluate Eq. (5) to leading order in $p_F l$, we find it convenient to express the Green functions as

$$\mathcal{G}^\pm(\epsilon, H) = \partial_\epsilon \ln(\epsilon^\pm - \mathcal{H}). \quad (6)$$

The advantage of this seemingly complicated representation will become apparent below. Expanding Eq. (6) in terms of V and taking only diagrams with avoided crossings of impurity lines, i.e., diagrams of leading order in p_F , into account, we are led to the result

$$\begin{aligned} K(\epsilon_1, H_1; \epsilon_2, H_2) &= \frac{\Delta^2}{2\pi^2} \partial_{\epsilon_1}^2 \partial_{\epsilon_2} \text{Re} \left[\sum_{n=2}^{\infty} \frac{1}{n} [S_n^{(D)}(\epsilon_1 - \epsilon_2, H_-) \right. \\ &\quad \left. + S_n^{(C)}(\epsilon_1 - \epsilon_2, H_+) \right. \\ &\quad \left. + S_1(\epsilon_1 - \epsilon_2) \right], \end{aligned} \quad (7)$$

where $H_\pm = H_1 \pm H_2$. Diagrammatically, the terms $S_n^{(C,D)}$ can be represented as

$$\begin{aligned} S_n^{(D)} &= \left[\text{Diagram with } n \text{ impurity lines, inner ring } G^+(\epsilon_1, H_1), \text{ outer ring } G^-(\epsilon_2, H_2) \right], \\ S_n^{(C)} &= \left[\text{Diagram with } n \text{ impurity lines, inner ring } G^+(\epsilon_1, H_1), \text{ outer ring } G^-(\epsilon_2, H_2) \right], \end{aligned} \quad (8)$$

where the inner and the outer ring are mutually connected by n impurity lines. The solid arrows represent

impurity-averaged Green functions. In coordinate representation

$$\begin{aligned} \underline{r} \quad (\epsilon, \pm) \quad r' \\ = \langle \mathcal{G}^\pm(\epsilon, H; r, r') \rangle \\ \equiv G^\pm(\epsilon, H; r, r') \\ = \left\langle r \left| \left[\epsilon \pm \frac{i}{2\tau} - H_0 \right]^{-1} \right| r' \right\rangle. \end{aligned} \quad (9)$$

In the diagrams S_2 and S_1 the relative direction of the arrows is meaningless, i.e., it is not necessary to distinguish between (D)- and (C)-type contributions. Introducing the quantities

$$\begin{aligned} \zeta^{(D)}(\omega, H_-; r, r') &= \frac{\Delta}{2\pi\tau} G^+(\epsilon_1, H_1; r, r') G^-(\epsilon_2, H_2; r', r), \\ \zeta^{(C)}(\omega, H_+; r, r') &= \frac{\Delta}{2\pi\tau} G^+(\epsilon_1, H_1; r, r') G^-(\epsilon_2, H_2; r, r'), \end{aligned} \quad (10)$$

where $\omega \equiv \epsilon_1 - \epsilon_2$ the diagrams $S_n^{(C,D)}$ can analytically be represented as

$$S_n^{(C,D)} = \frac{1}{L^{nd}} \int \prod_{m=1}^n dr_j \prod_{m=1}^n \zeta^{(C,D)}(r_m, r_{m+1}), \quad r_{n+1} \equiv r_1. \quad (11)$$

The analysis of the right-hand side (rhs) of this equation can be formulated in a much more transparent way if we regard the $\zeta^{(C,D)}$ as linear integral operators with coordinate representation $\zeta^{(C,D)}(r, r')$. Then

$$S_n^{(C,D)} = \text{tr}[\zeta^{(C,D)}]^n \quad (12)$$

and

$$\begin{aligned} K(\omega, H_1, H_2) \\ = -\frac{\Delta^2}{2\pi^2} \partial_\omega^2 \{ \text{tr} \hat{\ln}[1 - \zeta^{(D)}(\omega, H_-)] \\ + \hat{\ln}[1 - \zeta^{(C)}(\omega, H_+)] - S_1(\omega) \}, \end{aligned} \quad (13)$$

where the function $\hat{\ln}$ is defined by the power series

$$\hat{\ln}(1-x) = -\sum_{n=2}^{\infty} \frac{1}{n} x^n = \ln(1-x) + x, \quad (14)$$

and can be handled like a conventional logarithm as long as the subtraction of the first-order contribution is understood. Apart from a few exceptional cases, the single-impurity scattering contribution S_1 does not play a significant role. At any rate, it deserves a special treatment; hence we have singled it out in Eq. (13) and discuss it separately in Appendix B.

As is obvious from Eq. (13), the spectral correlation function is essentially determined by the eigenvalues of the integral operator ζ . This is the main advantage of representing K in terms of energy derivatives of the diagrams S_i . Expanding the Green functions entering Eq. (5) directly, rather than their logarithm, leads to diagrams of more complicated structure containing vertex parts in addition to the impurity ladders.¹³ In order to

discuss these diagrams, one has to calculate expressions involving both Green functions and the *eigenfunctions* of the operator ζ . This entanglement, while inessential in the diffusive cases, leads to major complications in the nondiffusive regimes. Furthermore, representing K as an energy derivative of some other function renders the energy integrations necessary to obtain Σ_2 trivial. This turns out to be essential as soon as we are going to consider energy windows E larger than the inverse scattering time. In that case, the integration domain splits into various regions in which the correlation function behaves qualitatively different. To a large extent the respective contributions to the integral tend to cancel each other, hence the result depends sensitively on the matching procedure between the different domains. On the other hand, the directly calculated correlation function is known only approximately, which renders a continuous matching and thereby makes the integration impossible.

We now turn to the discussion of the operators ζ . Both their eigenvalues and eigenfunctions depend on the shape and dimensionality of the sample and, in particular, on the characteristics of the magnetic field. In the present section we shall consider the comparatively simple case of a $2d$ quadratic sample *in the absence of a magnetic field*. No current is allowed to flow across the boundaries, i.e., we have to impose Dirichlet conditions on the Green functions entering Eq. (10). In an eigenfunction decomposition,

$$\begin{aligned} G^\pm(\epsilon, r, r') &= \sum_p t(p, r) D^\pm(\epsilon, p) t(p, r'), \\ D^\pm &= \left[\epsilon \pm \frac{i}{2\tau} - \frac{1}{2m} p^2 \right]^{-1}, \end{aligned} \quad (15)$$

$$\begin{aligned} t(p, r) &= \frac{2}{L} \sin(p_1 r_1) \sin(p_2 r_2), \\ p_i &= \frac{n_i \pi}{L}, \quad n_i = 1, 2, \dots, \end{aligned}$$

where L is the sample length, $r = (r_1, r_2)$ and \sum_p is an abbreviation for the summation over all modes n_i . The diagonalization of the thus defined ζ , i.e., the solution of the integral equation

$$\frac{1}{L^d} \int dr' \zeta(\omega; r, r') \psi_q(r') = \lambda(q, \omega) \psi_q(r) \quad (16)$$

is discussed in Appendix A. As a result, we obtain the eigenfunctions

$$\begin{aligned} \psi_q(r) &= \prod_{i=1,2} a_{q_i} \cos(q_i r_i), \quad q_i = \frac{m_i \pi}{L}, \quad m_i = 0, 1, \dots, \\ a_{q_i} &= \begin{cases} L^{-1/2}, & q_i = 0 \\ L^{-1/2} \sqrt{2}, & q_i \neq 0 \end{cases} \end{aligned} \quad (17)$$

with associated eigenvalues¹⁴

$$\lambda(q, \omega) = [(1 + i\omega\tau)^2 + (ql)^2]^{-1/2}, \quad (18)$$

where $q = \sqrt{q_1^2 + q_2^2}$. Substituting the $\lambda(q, \omega)$ in Eq. (13) and noticing that in the field-free case no distinction

between $\xi^{(D)}$ and $\xi^{(C)}$ is necessary, we are led to the provisional results

$$K(\omega) = \frac{\Delta^2}{2\pi^2} \partial_\omega^2 \left[2 \sum_q \widehat{\ln}[1 - \lambda(q, \omega)] - S_1(\omega) \right] \quad (19)$$

and

$$\Sigma_2(E) = \frac{1}{\pi^2} \text{Re} \sum_q \{ 2 \widehat{\ln}[1 - \lambda(q, E)] - 2 \widehat{\ln}[1 - \lambda(q, 0)] - [S_1(E) - S_1(0)] \}. \quad (20)$$

As is indicated by the form of the $\lambda(q, \omega)$, all further steps in the evaluation of Eqs. (19) and (20) depend on the correlation range ω and (via the quantization conditions to be imposed on the modes q) the system size. As for the system size, the two alternatives $L \gg l$ and $L \ll l$ have to be distinguished. We begin by considering the diffusive case, $L \gg l$.

A. Diffusive systems $L \gg l, H=0$

In this case, three energy regimes with qualitatively different spectral statistics can be identified:

$$\begin{aligned} D1: & 0 \leq \omega < E_c, \\ D2: & E_c < \omega < 1/\tau, \\ D3: & 1/\tau < \omega. \end{aligned} \quad (21)$$

The meaning of this partition of the energy axis can be understood by interpreting the spectral correlation function semiclassically. According to Ref. 8,

$$K(t) \propto tP(t), \quad (22)$$

where $K(t)$ is the energy Fourier transform of $K(\omega)$ and $P(t)$ denotes the classical probability for periodic motion, i.e., the probability that a classical particle released at time $t=0$ somewhere in the system returns to its initial *phase-space* coordinates after time t . In this interpretation, regime *D1* corresponds to times larger than the diffusion time E_c^{-1} through the system, which implies that the probability density for finding the particle at an arbitrary point has equilibrated to some constant value. In the intermediate time domain ($\cong D2$) the particle is moving diffusively in a region close to its initial point. Finally, regime *D3* represents times comparable with the scattering time, i.e., the corresponding classical dynamics is governed by free motion, eventually interrupted by a few scattering events.

The small energy regimes *D1* (Ref. 15) and *D2* (Ref. 13) have been investigated earlier and we discuss them only for the sake of completeness. For $\omega < E_c$, the constant mode $q=0$ dominates the sum in Eq. (20). This reflects the spatial equilibration of classical and quantum probability density after sufficiently long times. Retaining only the zero mode, we obtain

$$\begin{aligned} D1: & K(\omega) = \frac{\Delta^2}{\pi^2} \frac{\gamma^2 - \omega^2}{(\gamma^2 + \omega^2)^2}, \\ & \Sigma_2(E) = \frac{1}{\pi^2} \ln \left[\frac{E^2 + \gamma^2}{\gamma^2} \right]. \end{aligned} \quad (23)$$

For times smaller than $(E_c)^{-1}$ the contribution of nonzero modes must no longer be neglected. The q -dependent eigenvalues differ significantly from zero as long as $(ql)^2 - (\omega\tau)^2 = O(\max[1, \omega\tau])$. In the diffusive regime this condition is met by $O(L/l)^2 \gg 1$ modes, hence it is permitted to replace the sum by an integral. Performing the integration, we obtain

$$K(\omega) = -\frac{2}{\pi} \left[\frac{L}{2\pi l} \right]^2 \text{Re} I(1 + i\omega'\tau) \Big|_{\omega'=0}^{\omega'=\omega}, \quad (24)$$

where

$$I(x) \equiv \frac{1}{2} [(x^2 - 1) \ln(x - 1) - x^2 \ln(x) + x]. \quad (25)$$

For energies smaller than the inverse scattering time, an expansion in the small parameter $\omega\tau$ yields^{13,16}

$$\begin{aligned} D2: & K(\omega) \simeq \frac{2(\Delta\tau)^2}{\pi} \left[\frac{L}{2\pi l} \right]^2 \ln(\omega\tau), \\ & \Sigma_2(E) \simeq \left[\frac{L}{2\pi l} \right]^2 E\tau. \end{aligned} \quad (26)$$

Note that the expressions appearing on the rhs of these equations are the respective leading-order contributions. The result given for K stems from the twofold energy derivative of a higher-order correction (in $\omega\tau$) to Σ_2 , which is not displayed. In the regime of large energies $\omega\tau \gg 1$,

$$\begin{aligned} D3: & K(\omega) = -\frac{1}{2\pi} \left[\frac{L}{2\pi l} \right]^2 \frac{\Delta^2}{\omega^2}, \\ & \Sigma_2(E) = \frac{1}{\pi} \left[\frac{L}{2\pi l} \right]^2 \ln(E\tau). \end{aligned} \quad (27)$$

In contradistinction to Ref. 13, where a saturation of the level number fluctuation towards a constant value for energies larger than the inverse scattering time was conjectured, we arrive at a logarithmically increasing expression for Σ_2 .¹⁷ This result, however, deserves further investigation as it depends nonuniversally on the microscopic features of the white-noise potential. The implications of different choices for the scattering potential will be discussed in Sec. III. Here we restrict ourselves to drawing a relation between the heuristic interpretation of regime *D3* given above and the Green-function formulation underlying the expression Eq. (20). In the regime of large energies, the rhs of Eq. (20) is dominated by the term that decays slowest in energy, i.e.,

$$\Sigma_2(E) \stackrel{E \gg 1/\tau}{\simeq} -\frac{1}{\pi^2} \text{Re} \sum_q [\lambda^2(q, E) - \lambda^2(q, 0)]. \quad (28)$$

Diagrammatically, this contribution can be represented as

$$\lambda(q, \omega)^2 \sim \sum_q \int d^2p d^2p' \quad \begin{array}{c} \text{---} p \text{---} \text{---} p' \text{---} \\ \text{---} G^+(\epsilon_1, H_1) \text{---} \\ \text{---} p' + q \text{---} \end{array} \quad , \quad (29)$$

$G^-(\epsilon_2, H_2)$

where the momentum dependence of all Green functions is indicated explicitly. Heuristically, the diagram describes a bouncing trajectory between two impurities. It is clear that Eq. (29) depends sensitively on the features of the scattering potential. In the general case of potentials with finite correlation length, the impurity lines have to be supplemented by form factors depending on the momentum exchange $p - p'$. As is detailed in Sec. III, this imposes restrictions on the momentum integrations and may lead to a qualitatively different q and ω dependence of the diagram, i.e., to a different large-energy behavior of the correlation functions. In Fig. 1 we have plotted Σ_2 of a diffusive sample over all three energy regimes.

B. Ballistic samples $L \ll l, H=0$

As in the diffusive case, three different energy regimes have to be distinguished:

$$\begin{aligned} B1: & 0 \leq \omega < 1/\tau, \\ B2: & 1/\tau < \omega < v_f L^{-1}, \\ B3: & v_f L^{-1} < \omega. \end{aligned} \quad (30)$$

On time scales corresponding to regime B1 the electrons are multiply scattered, i.e., their motion is diffusive. In contradistinction to the previously considered case $L \gg l$, however, these times are at any rate larger than the time

of flight through the system, which means that the energy scale E_c no longer plays the role of the inverse diffusion time through the system. The existence of regime B2, corresponding to times smaller than the scattering time but larger than the time of flight L/v_f through the system, motivates the denotation ballistic samples. Regime B3 represents times shorter than the time of flight. Contrary to the diffusive case, disorder-induced spectral correlations in the ballistic regime depend in general on the system geometry. Strictly speaking, our analysis applies to two-dimensional systems of square (or slightly more general, of rectangular) geometry. Nevertheless, it is obvious on physical grounds that the result obtained in regime B1 (where electrons scatter multiply off impurities) is insensitive against changes in the underlying system geometry.

For energies smaller than $v_f L^{-1}$, i.e., in regimes B1 and B2, the constant mode $q=0$ dominates the sum over eigenvalues, Eq. (19) (a similar statement was made above for diffusive systems; cf. Fig. 2, which demonstrates this fact for a marginally ballistic system, $2\pi l/L=2$). In light of the interpretation given above, this reflects the fact that the time of flight L/v_f rather than the diffusion time $(E_c)^{-1}$ determines the transport time through a ballistic sample. Retaining only the zero mode and neglecting terms of higher order in $\omega\tau \ll 1$, we obtain in regime B1, like in D1,

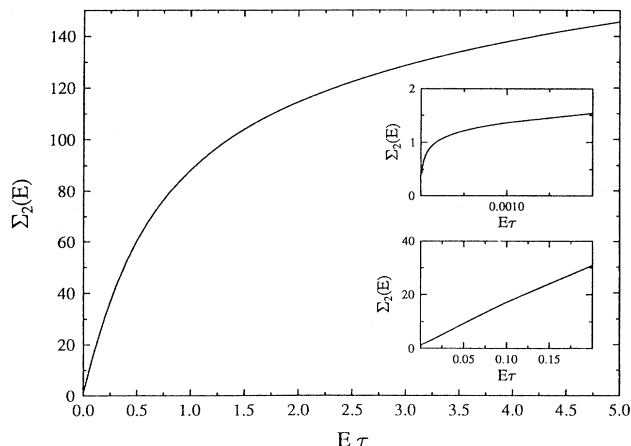


FIG. 1. $\Sigma_2(E)$ in the diffusive case ($p_F l = 100, L/l = 10$).

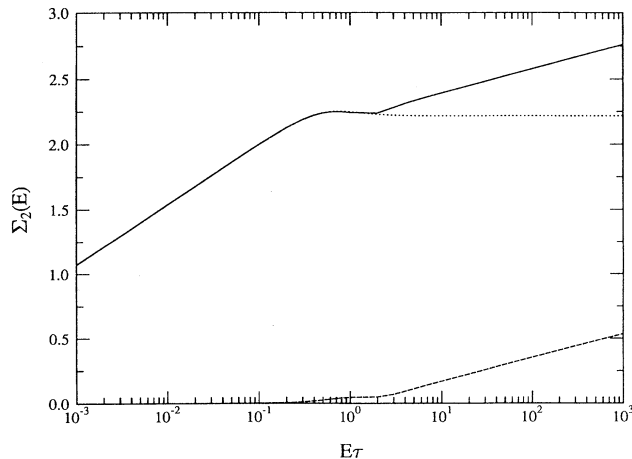


FIG. 2. Semilogarithmic plot of Σ_2 for a sample with $2\pi l/L=2$. Zero-momentum mode (dotted line) and S_2 contribution (broken line) are displayed separately (cf. the text).

$$B1: K(\omega) = \frac{\Delta^2}{\pi^2} \frac{\gamma^2 - \omega^2}{(\gamma^2 + \omega^2)^2}, \quad (31)$$

$$\Sigma_2(E) = \frac{1}{\pi^2} \ln \left[\frac{E^2 + \gamma^2}{\gamma^2} \right].$$

As soon as ω becomes larger than $1/\tau$, the contribution of nonzero modes $q \neq 0$ in Eq. (19) can no longer be neglected though it is still exceeded by the 0-mode term.

$$K(\omega) = \frac{\Delta^2}{2} \partial_\omega^2 \left[\frac{1}{\pi^2} \ln \left[\frac{\omega^2 + \gamma^2}{\gamma^2 [1 + (\omega\tau)^2]} \right] - \frac{2}{\pi^2} \frac{(\omega\tau)^2}{1 + (\omega\tau)^2} - \frac{4}{\pi} \left[\frac{L}{2\pi l} \right]^2 \text{Re} I \left\{ \left[(1 + i\omega\tau)^2 + \left[\frac{2\pi l}{L} \right]^2 \right]^{1/2} \right\} \right], \quad (32)$$

where the function I is defined in Eq. (25). In *B2* one obtains

$$B2: K(\omega) = \frac{3\Delta^2}{2\pi^2\tau^2} \frac{1}{\omega^4}, \quad (33)$$

$$\Sigma_2(E) = -\frac{2}{\pi^2} \ln(\gamma\tau) - \frac{2}{\pi^2} \frac{(E\tau)^2}{1 + (E\tau)^2}.$$

The most remarkable feature of this result is the non-monotony of Σ_2 as a function of energy, which implies that the fluctuations in the number of levels contained in energy windows of width $\tau^{-1} < E < v_f L^{-1}$ decrease upon increasing the width of the energy interval.

For energies much larger than $v_f L^{-1}$, Σ_2 increases logarithmically like in regime *D3*,

$$B3: K(\omega) \xrightarrow{\omega \gg v_f L^{-1}} -\frac{1}{2\pi} \left[\frac{L}{2\pi l} \right]^2 \left[\frac{\Delta}{\omega} \right]^2, \quad (34)$$

$$\Sigma_2(E) \xrightarrow{E \gg v_f L^{-1}} \frac{1}{\pi} \left[\frac{L}{2\pi l} \right]^2 \ln(E\tau).$$

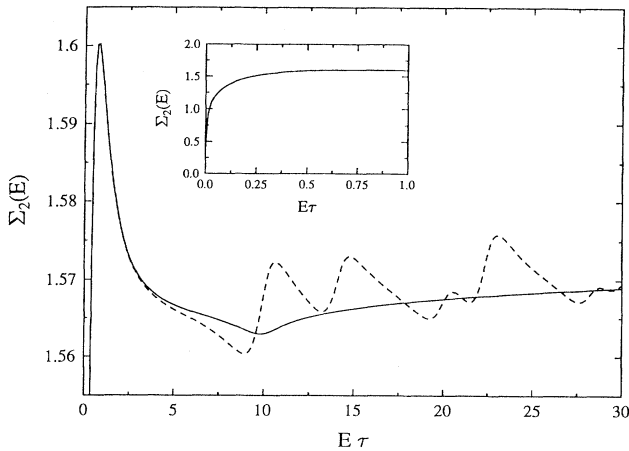


FIG. 3. $\Sigma_2(E)$ in the ballistic case ($p_f l = 10^4$, $L/l = 0.1$). The dashed line corresponds to the numerically evaluated sum (20), while the solid line corresponds to the approximation (32).

In contradistinction to the diffusive case, however, only a few modes contribute significantly to the sum over eigenvalues for each particular choice of ω . A replacement of the q sum by an integral can therefore be no more than a crude approximation of the exact value. Its accuracy can be improved by singling out the constant mode (the first two terms on the rhs of the expression below) and replacing only the sum over modes $q \neq 0$ by an integral with lower cutoff $2\pi/L$. Performing the integration we obtain

This result comes as no surprise since for energies much larger than the inverse time of flight the features of the bulk sample rather than the boundaries should determine the behavior of the correlation functions.

In Fig. 3 we have plotted the analytical result Eq. (32) (solid line) together with the numerically evaluated sum Eq. (19) (dashed line). While both results coincide in regimes *B1* and *B2*, the numerically obtained curve exhibits fluctuations around the analytical result in regime *B3*. Similar fluctuations have been found in the energy correlation functions of chaotic stadium billiards with parallel sections.¹⁸ Semiclassically, they may be interpreted as due to the existence of short periodic orbits connecting opposite parallel boundaries. It is therefore natural to expect that the characteristic energy scale associated with the oscillations shown in Fig. 3 is given by the inverse time of flight. This conjecture can be confirmed by analyzing Eq. (19) by means of a two-dimensional generalization of the Poisson sum rule. The resulting expressions, however, are little transparent whence we do not display them explicitly.

III. NONUNIVERSALITY

As has been argued qualitatively in Sec. II, the spectral correlation functions exhibit nonuniversal behavior on energy scales that are large in comparison with the inverse scattering time. In this section we investigate in more detail how the microscopic features of the scattering potential affect the spectral statistics. To be specific, we discuss the generalization of the potential correlator Eq. (1) to a finite correlation length a ,

$$\langle V(x)V(y) \rangle = v^2 e^{-(x-y)^2/a^2}. \quad (35)$$

To compare Eqs. (1) and (35), the potential strength v should be expressed in terms of the resulting scattering time τ at the Fermi surface. In the first Born approximation the scattering time of an electron moving with momentum $p = O(p_f)$ is given by

$$\tau^{-1} = 2 \left[\frac{L}{2\pi} \right]^2 \int d^2 p' F(p-p') \text{Im} G^-(p'), \quad (36)$$

where F is the Fourier transform of the potential correlator

$$\begin{aligned} F(p) &= L^{-2} \int d^2x \langle V(x)V(0) \rangle e^{ipx} \\ &= \pi \left[\frac{va}{L} \right]^2 e^{-(1/2)p^2 a^2}. \end{aligned} \quad (37)$$

Performing the momentum integration, we obtain

$$\begin{aligned} \tau^{-1} &= 2\pi v v^2 f(a), \\ f(a) &\equiv \frac{a^2}{2} \int_0^{2\pi} d\theta e^{-(ap_F)^2(1-\cos\theta)}. \end{aligned} \quad (38)$$

As is obvious from Eq. (37), the finiteness of the correlation length leads to an exponential suppression

$\propto \exp[-(\Delta p a)^2]$ of the momentum transfer Δp per scattering event. For energies much smaller than the transport scattering time τ_{tr}^{-1} , this phase-space restriction does not lead to qualitative changes in the spectral correlations. On the corresponding time scales the particle's motion can be compared with a long random walk and details of individual scattering processes average out. These qualitative statements can be put in a more rigorous form by proving that the finiteness of the potential range does not alter the singularity of the diffusion pole. In the opposite case $E > 1/\tau > 1/\tau_{tr}$ the two-impurity scattering process S_2 represented in Eq. (29) gives the dominant contribution to the correlation functions. Substituting Eq. (37) for the scattering lines and noticing that only momenta close to the Fermi surface contribute significantly to the integration, we obtain

$$\begin{aligned} S_2(q, \epsilon_1 - \epsilon_2) &= \left[\frac{\pi}{2\pi v \tau f(a)} \left[\frac{a}{2\pi} \right]^2 \right]^2 \int d^2p d^2p' e^{-(p_F a)^2(1-\cos\theta)} G^+(\epsilon_1, p) G^+(\epsilon_1, p') G^-(\epsilon_2, p+q) G^-(\epsilon_1, p'+q), \\ &\theta = \angle(p, p') \end{aligned} \quad (39)$$

for the analytical expression corresponding to the diagram Eq. (29). Let us discuss Eq. (39) in the respective limiting case $p_F a \ll 1$ and $p_F a \gg 1$ separately. If $p_F a \ll 1$, the factor $\exp[-(p_F a)^2(1-\cos\theta)]$ can be replaced by unity and we obtain the same result as in the white-noise case, i.e.,

$$S_2(\omega)^{p_F a \ll 1} \xrightarrow{\omega \tau \gg 1} \frac{1}{2\pi} \left[\frac{L}{2\pi l} \right]^2 \ln(\omega \tau). \quad (40)$$

This does not come as a surprise since the mean extension a of the scattering centers is much smaller than the typical wavelength of the electrons, hence the scattering can be regarded as effectively pointlike.

Let us now turn to the opposite limit of a soft potential $p_F a \gg 1$. In this case, the angle-dependent suppression factor forces p and p' to be close to each other and we may expand in terms of small angular deviations θ . As a result of a straightforward integration, we obtain

$$\begin{aligned} S_2(\omega)^{p_F a \gg 1} \xrightarrow{\omega \tau \gg 1} \pi^{1/2} p_F a \left[\pi \left[\frac{L}{2\pi l} \right]^2 \right. \\ \left. + 2 \operatorname{Re}(1 + i\omega \tau)^{-2} \right]. \end{aligned} \quad (41)$$

Equations (40) and (41) imply a nonuniversal dependence of the correlation functions on the microscopic features of the disorder in the regime of large energies. The summed contribution of all higher-order diagrams S_n , $n \geq 3$ gives a finite contribution to the correlation functions as E becomes large. Hence, the logarithmic divergence exhibited by $S_2^{p_F a \ll 1}$ implies a logarithmic diver-

gence of Σ_2 as a whole (cf. Figs. 1 and 3). In the opposite case of a soft potential, however, S_2 converges, which means that Σ_2 saturates at a constant value with increasing E . A reliable estimation of the limiting value is difficult as it would necessitate a calculation of higher-order diagrams S_n ; $n \geq 3$ in the presence of a soft potential for intermediate energies $1/\tau < \omega < 1/\tau_{tr}$. It is also instructive to study the sensitivity of the short time return probability against the properties of the scattering potential. In the white-noise case, Fourier transformation of $S_2(\omega)$ leads to

$$P(t)^{p_F a \ll 1} \xrightarrow{t \ll \tau} \text{const} \times \left[\frac{L}{2\pi l} \right]^2. \quad (42)$$

At first sight, the nonvanishing of $P(t)$ as t approaches 0 may seem to be paradoxical. It can be explained by noticing that the white-noise correlator Eq. (1) represents a dense distribution of hard (*s*-wave) scatterers, i.e., arbitrary small surroundings of a given initial point still contain impurities that act as backscattering centers. In the opposite case $p_F a \gg 1$, however, the return probability vanishes,

$$P(t)^{p_F a \gg 1} \xrightarrow{t \ll \tau} \text{const} \times p_F a \frac{t}{\tau}, \quad (43)$$

indicating that the softness of the potential lowers the efficiency of the backscattering.

IV. FEATURES OF THE CLEAN SPECTRUM AFFECTING THE CORRELATION FUNCTION

So far we have neglected the fact that even the spectrum of a clean square exhibits nontrivial spectral correlations. In the diffusive case, the level structure of the clean sample indeed turns out to be inessential. As soon as $L \sim l$, however, one encounters a subtle interplay between the spectral statistics of the clean sample on the one hand and disorder-induced spectral correlations on the other hand. Before turning to a discussion of this point let us review some features of the clean spectrum and their robustness against a moderate amount of disorder.

A clean square sample possesses two intrinsic energy scales: The level spacing Δ and the inverse time of flight t_f^{-1} . Energy correlations on small scales $\Delta E \ll t_f^{-1}$ have previously been investigated in numerous works.^{11,19} For our purpose, however, the large-scale properties are of primary importance. In order to reveal the existence of long-range fluctuations in the density of states, it is convenient to coarse grain the spectrum over short distances. Equivalently one may assign an imaginary width $\gamma \gg \Delta$ to individual levels by configurational averaging: Introducing some amount of disorder, which mixes the unperturbed levels E_n over scales $1/\tau$ with $\Delta \ll 1/\tau < t_f^{-1}$, and averaging over all its microscopic realizations leads to the appearance of a width $E_n \rightarrow E_n + i/(2\tau) \equiv E_n^+$. We are thus led to investigate

$$\begin{aligned} \langle \nu(E_F) \rangle &= \frac{1}{\pi L^2} \text{Im} \langle \text{tr} [G^-(E_F)] \rangle \\ &\simeq \frac{m}{\pi L^2 p_F l} \sum_p \frac{1}{(p - p_F)^2 + (2l)^{-2}}. \end{aligned} \quad (44)$$

In the last equation we have linearized the spectrum around E_F , exploiting the fact that $E_F \gg \tau^{-1}$. Qualitatively, the E_F dependence (i.e., the p_F dependence) of $\langle \nu(E_F) \rangle$ can be foreseen by inspecting the weight $f(p, p_F) \equiv [(p - p_F)^2 + (2l)^{-2}]^{-1}$ in the two-dimensional space of discrete modes p . The function f may be visualized as a ring of width $1/l$ and radius p_F . In the diffusive regime, $1/l$ exceeds the intermode spacing $2\pi/L$ and the number of intermixed levels can accurately be estimated by dividing the ring's area $2\pi p_F l$ by the area per mode $(2\pi/L)^2$. As a result, one obtains the constant density of states $\langle \nu(E_F) \rangle \equiv \bar{\nu} = m/(2\pi)$. Upon approaching the ballistic case, however, the width of the ring shrinks

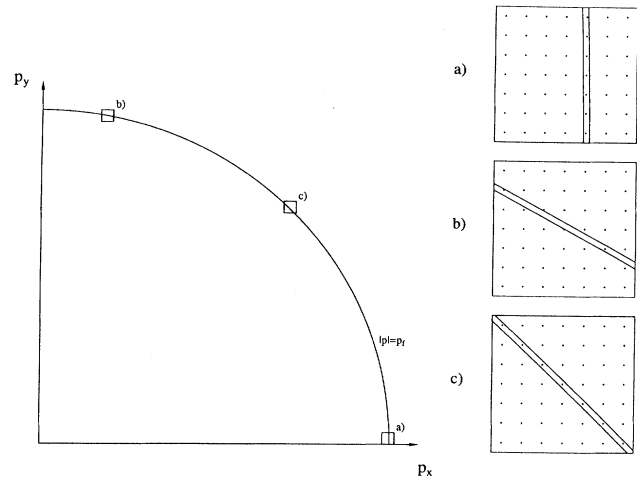


FIG. 4. Schematic plot of the Fermi ring characterizing a ballistic sample (cf. the text).

below the intermode spacing [cf. Fig. 4(b)] and one may expect the onset of fluctuations in $\langle \nu \rangle$. In particular, one encounters exceptional situations where $f(p_F)$ cuts a line of levels [cf. Figs. 4(a) and 4(c)], in which case the number of levels included in the ring changes drastically. A simple geometric construction leads to $\delta \langle \nu \rangle \sim \langle \nu \rangle [l/(p_F L^2)]^{1/2}$ as an estimate for the excess number of states in such resonant scenarios. The typical spacing between consecutive sudden changes in the number of levels is $\delta p_F \sim (\pi/L)$ corresponding to $\delta E_F \sim \pi t_f^{-1}$ for the period of oscillations in $\nu(E \simeq E_F)$.

In order to incorporate the phenomenon of these fluctuations in a quantitative description of spectral correlations, one has to calculate the sum Eq. (44) rigorously. For this purpose, we employ a two-dimensional generalization of the Poisson sum rule and write

$$\langle \nu(E_F) \rangle = \frac{1}{4\pi^3} \sum_k \int d^2 p e^{i\mathbf{p} \cdot \mathbf{L}_k} \text{Im} \frac{1}{E_F^+ - p^2/2m}, \quad (45)$$

where $\mathbf{L}_k^T = 2L(k_1, k_2)$, $k_i = 0, \pm 1, \dots$ is a two-dimensional vector, and the angular brackets denote a configurational average at fixed sample size. The latter condition will become of importance below. Introducing polar coordinates and integrating over the modulus of p , we arrive at

$$\begin{aligned} \langle \nu(E_F) \rangle &= \frac{m}{2\pi} \left[1 + \frac{1}{2\pi} \sum_{k \neq 0} \int_0^{2\pi} d\theta \exp \left[iL_k p_F \cos\theta - \frac{L_k}{2l} |\cos\theta| \right] \right] \\ &\simeq \frac{m}{2\pi} \left[1 + \sum_{k \neq 0} \left[\frac{2}{\pi L_k p_F} \right]^{1/2} \cos(L_k p_F - \pi/4) e^{-L_k/2l} \right], \end{aligned} \quad (46)$$

where $L_k = |\mathbf{L}_k|$. In Fig. 5 we have plotted $\langle \nu(E_F) \rangle$ for several values of the disorder. Spacing and amplitude of the fluctuations agree with the qualitative estimate given above.

For the sake of future reference, let us now investigate correlations in the energy-dependent quantity $\langle \nu(E) \rangle$ and calculate

$$K'(\omega) \equiv \frac{1}{\bar{v}^2} [\langle \langle v(E+\omega) \rangle \langle v(E) \rangle \rangle_{E_0} - \langle \langle v(E+\omega) \rangle \rangle_{E_0} \langle \langle v(E) \rangle \rangle_{E_0}], \quad (47)$$

where $\langle \rangle_{E_0}$ denotes averaging in E over an interval of width $t_f^{-1} \ll E_0 \ll E_F$ centered at the Fermi energy, e.g.,

$$\langle F(E) \rangle_{E_0} \equiv \frac{1}{\pi^{1/2} E_0} \int_{-\infty}^{\infty} dE e^{-(E-E_F)^2/E_0^2} F(E). \quad (48)$$

Expanding $p(E) \simeq p_F + (E - E_F)/v_f + O(p_F(E_0/E_F)^2)$, we have

$$\langle e^{iL_k p(E)} \rangle_{E_0} = O(e^{-E_0 t_f^2}) \ll 1,$$

from which we obtain with exponential accuracy

$$K'(\omega) = \frac{2}{\pi} \sum_{k, k' \neq 0} \frac{1}{p_F (L_k L_{k'})^{1/2}} e^{-(L_k + L_{k'})/(2l)} \langle \cos[L_k p(E + \omega) - \pi/4] \cos[L_{k'} p(E) - \pi/4] \rangle_{E_0}. \quad (49)$$

Due to the suppression factors $\sim \exp(-L_k/l)$ the k summations are cut off at $L_k = O(l)$. For values $L_k, L_{k'} = O(l)$, a lower bound for $|L_k - L_{k'}|$, $L_k \neq L_{k'}$, can roughly be estimated as L^2/l . Energy averaging such nearby values leads to

$$|\langle e^{i(L_k - L_{k'}) p(E)} \rangle_{E_0}| \leq O(e^{-E_0 t_f L/l}), \quad k \neq k'$$

i.e., for sufficiently large

$$E_0 > l/(L t_f) \quad (50)$$

contributions with $k \neq k'$ are negligible and we arrive at

$$K'(\omega) = \frac{1}{\pi} \sum_{k \neq 0} \frac{1}{p_F L_k} e^{-L_k/l} \cos\left[\frac{L_k}{v_f} \omega\right]. \quad (51)$$

For energy differences $\omega \ll v_f L^{-1}$, the sum may be replaced by an integral leading to

$$K'(\omega) \simeq \frac{2}{p_F l} e^{-L/l} \frac{1}{(L/l)^2 + (\omega t_f)^2}. \quad (52)$$

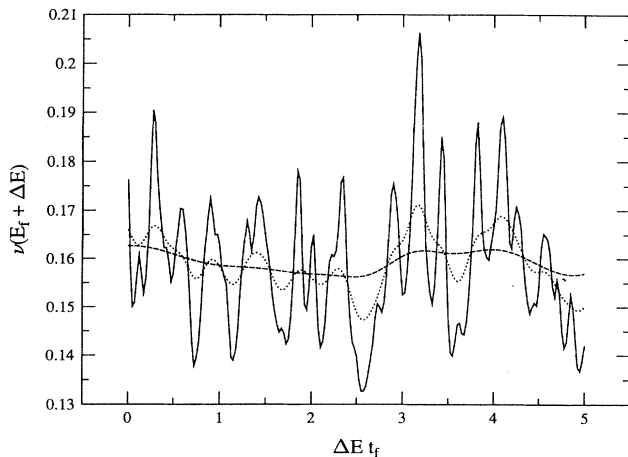


FIG. 5. Density of states plotted for various values of the disorder. $p_F L = 1000$, $m = 1$. Solid line, $l/L = 10$; dotted line, $l/L = 3$; broken line, $l/L = 1$.

In Fig. 6, we have plotted the numerically evaluated sum Eq. (51) for various values of the disorder. The density-of-states fluctuations discussed above lead to the appearance of cusps in the correlation function on energy scales $\omega > v_f L^{-1}$. While the height of these cusps is determined by the amount of disorder, their width and position depend on the system geometry, indicating that we are probing a nongeneric regime.

Before concluding this section, let us comment on the role of system-size fluctuations in connection with the ensemble average. Above we argued that the ensemble-averaged density of states exhibits fluctuations. Inspection of Eq. (44), however, shows that the fluctuation pattern depends sensitively on the system size L : Even a minute change in L of order $\delta L = O(p_F^{-1})$ leads to a drastic change in the energy dependence of ν . On the other hand, the correlation function K' seems to be comparatively insensitive against variations of L . These observations suggest one should consider two alternative averaging procedures, both being of practical relevance.

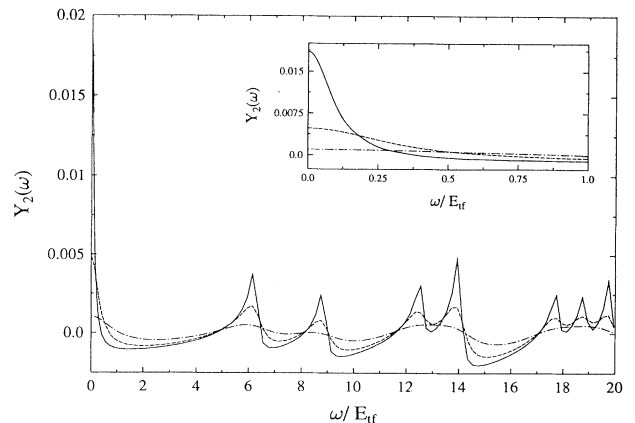
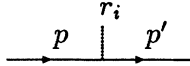


FIG. 6. The energy correlation function Eq. (51) (here denoted by Y_2) plotted for various values of the disorder. $p_F L = 1000$, $m = 1$. Solid line, $l/L = 10$; broken line, $l/L = 3$; dash-dotted line, $l/L = 1$.

(a1) Keep the system boundary strictly fixed upon averaging over realizations of a certain type of disorder.

(a2) Parametrize a set of systems containing, say, N impurities by their coordinates $r_i, i = 1, \dots, N$. The sizes of the systems may differ by a certain amount δL . For the sake of notational simplicity, we do not introduce δL_x and δL_y separately.

Scenario (a1) is the one we have considered so far. Let us now comment on (a2). Consider the diagrammatic expansion of some observable of interest. Obviously, any diagram containing unpaired impurities, e.g.,



will vanish as before upon averaging over the phase $\sim \exp[i(p - p')r_i]$ associated with the scattering. Moreover, in each diagram containing only paired impurities, the effective impurity interaction has to conserve momentum in order to prevent the appearance of large random phases. These observations impose restrictions on the class of significant diagrams *before* ensemble averaging. In particular, none of the relevant diagrams contains the impurity coordinates explicitly. The ensemble-dependent variations amount to different quantization conditions imposed by the varying system sizes $L + \delta L$ on the momentum summations. Neglecting fluctuations in the scattering time $1/\tau$ (which is a reasonable approximation as long as $\delta v \ll v$, i.e., $\Delta \ll 1/\tau$), we are again led to Eq. (46) for the density of states. Ensemble averaging amounts to averaging δL over a certain range. Since δL appears as a factor in a large phase, the fluctuating contribution to the density of states readily averages to zero and we conclude that $\langle v \rangle$ is constant as soon as we allow for tiny variations $\delta L > 1/p_F$. In the qualitative picture discussed above, sample-size fluctuations amount to a quenching and stretching of the momentum lattice. Since fluctuations $\delta L > 1/p_F$ are equivalent to fluctuations $\delta p_F > 1/L$ in the radius of the Fermi circle, the p_F -dependent structure of the density of states gets lost even for size variations on atomic scales. We note that averaging over the system size with $\delta L > 1/p_F$ such that $\delta E_F > 1/t_f$ is synonymous to energy averaging [cf. Eq. (48)] with $E_0 > 1/t_f$. Note that condition Eq. (50) leading to Eq. (51) is equivalent to system-size averaging with $\delta L > l/(p_F L)$.

Although the (a2)-averaged density of states is constant, one may still expect the presence of correlations in the spectrum, e.g., in individual samples the density of states at a given E will be correlated with the density of states at $E + v_j L^{-1}$. In the following section, the difference between (a1)- and (a2)-type correlations will be discussed in a somewhat more general context.

A. A unified treatment of disorder- and energy-averaged spectral correlations

We now turn to a unification of the previously found results. To this end, we characterize the spectral properties of our sample in terms of two correlation functions,

$$K^d(\omega) = \frac{1}{\bar{v}^2} \langle \langle v(E + \omega)v(E) \rangle \rangle_{\text{ens}} - \langle v(E + \omega) \rangle_{\text{ens}} \langle v(E) \rangle_{\text{ens}} \Big|_{E_0}, \quad (53)$$

$$K^E(\omega) = \frac{1}{\bar{v}^2} \langle \langle v(E + \omega)v(E) \rangle \rangle_{E_0} - \langle v(E + \omega) \rangle_{E_0} \langle v(E) \rangle_{E_0} \Big|_{\text{ens}},$$

where $\langle \dots \rangle_{\text{ens}}$ stands for ensemble averaging according to either procedure (a1) or (a2) and $\bar{v} \equiv \langle \langle v \rangle \rangle_{\text{ens}} \Big|_{E_0}$. Note that K^d and K^E differ from each other just by the sequence of disorder and energy average, respectively. Beginning with (a2), we consider the two averaging procedures introduced above separately. According to the previous section, (a2)-type averaging implies $\langle v(E) \rangle_{\text{ens}} = \bar{v} = \text{const}$, i.e.,

$$\langle \langle v(E + \omega) \rangle \rangle_{E_0} \langle v(E) \rangle_{E_0} \Big|_{\text{ens}} = \langle \langle v(E + \omega) \rangle \rangle_{\text{ens}} \langle v(E) \rangle_{\text{ens}} \Big|_{E_0} = \bar{v}^2.$$

Furthermore, disorder and energy averaging commute with each other such that we may conclude

$$(a2): K^d = K^E = \frac{1}{\bar{v}^2} \langle \langle v(E + \omega)v(E) \rangle \rangle_{\text{ens}} \Big|_{E_0} - 1. \quad (54)$$

Consider now the diagrammatic analysis of $\langle v v \rangle_{\text{ens}}$. One may distinguish between diagrams in which both factors are connected by impurity lines and an impurity-disconnected contribution. Commonly, the latter cancels against \bar{v}^2 . In our scenario (a2), however, this is not the case. The reason is, of course, that individual samples differ not only in the impurity constellation but also in their size. We thus obtain for the impurity-disconnected part $\langle v v \rangle_{\text{ens,nc}}$ Eq. (49), which is to be averaged over both sample sizes and energy. As in the previous section, this procedure leads to

$$\frac{1}{\bar{v}^2} \langle \langle v(E + \omega)v(E) \rangle \rangle_{\text{ens,nc}} \Big|_{E_0} = K'(\omega) + 1,$$

where K' is given by Eq. (51). We note that K' is exponentially small for $L > l$, rendering the present discussion for diffusive systems irrelevant. Combining this result with the impurity-connected contribution, we obtain

$$(a2): K^d(\omega) = K^E(\omega) = K(\omega) + K'(\omega), \quad (55)$$

where K is the previously calculated disorder correlation function [cf. Eq. (19)]. Comparison of the respective small-energy expansions, Eqs. (52) and (31), shows that for $\omega > \Delta(p_F L)^{1/2} L / l$ the disorder-connected contribution K is negligibly small.

The situation is different when (a1)-type averaging is performed, in which case K^d and K^E no longer equal each other. Still $\langle v \rangle_{E_0} = \bar{v}$, hence we have as in the (a2) case,

$$(a1): K^E(\omega) = K(\omega) + K'(\omega). \quad (56)$$

On the other hand, $\langle v \rangle$ is no longer constant [cf. Eq. (46)]. Since individual samples differ only in their impurity configuration, the impurity-disconnected contribution

to $\langle \nu \nu \rangle_{\text{ens}}$ cancels exactly against $\langle \nu \rangle_{\text{ens}} \langle \nu \rangle_{\text{ens}}$ and we obtain

$$(a1): K^d(\omega) = K(\omega). \quad (57)$$

From this discussion we conclude that in order to observe the (more interesting) disorder correlation function K for energies larger than $\Delta(p_F L)^{1/2} L/l$, one necessarily has to perform (a1)-type averaging. One may also speculate about the relevance of these results to experiments probing the existence of chaotic behavior in mesoscopic systems. In the context of quantum chaos, the energy correlation function K^E plays a crucial role. Drawing from the above discussion and according to Eqs. (55) and (56), its small energy structure is governed by the disorder-dependent contribution K , thereby always indicating the onset of chaotic behavior for sufficiently long time scales. The fine-scale structure of the clean spectrum, i.e., the long-time behavior of the semiclassical trajectories, will be masked by K . Evidently, our results do not apply to common practice quantum chaos experiments performed with mesoscopic systems. First, no disorder averaging [cf. the definition of K^E , Eq. (53)] needs to be performed in such experiments. Second, and more important, one will in general investigate geometries different from the square geometry, viz., geometries leading to chaotic motion. Nevertheless we believe that the unavoidable presence of disorder will render the motion eventually chaotic, thereby making the long-time distinction between chaotic and nonchaotic geometries impossible. The two most relevant parameters governing the competition between disorder and geometry-induced chaos are $1/\tau$ and the Lyapunov exponent characterizing the clean system.

Finally, we would like to stress that it is possible, in principle, to define other types of two-level correlation functions (permuting, for example, the order of impurity, energy, and size averaging). Our aim here was to discuss the most relevant, experimentally accessible cases.

V. FINITE MAGNETIC FIELDS

So far we have considered spectral statistics in field-free systems. Earlier on we have stated that our approach is applicable to situations where a static (and uniform) magnetic field is applied, as long as it is not too strong. Application of a magnetic field breaks invariance under time reversal. As long as the spectral statistics is described by random-matrix theory, this defines a GOE (Gaussian orthogonal ensemble) statistics to GUE (Gaussian unitary ensemble) statistics crossover. Evidently, this transition does not take place abruptly.²⁰ One may rather define a field-dependent energy scale E_H , such that on energy scales much smaller than E_H GUE statistics prevails, while correlations much larger than E_H are properly described by GOE statistics.^{1,2,20} This characterization, as it implies the validity of random-matrix theory is only suitable under ergodic conditions. On the other hand, one should expect that the energy scale E_H characterizes a crossover in the correlation function and derivatives thereof under much more general conditions as well. In order to pursue our analysis of

the field-dependent correlation function, we have to classify the various regimes not only according to disorder strength and energy scales (along the lines of Sec. II), but also with respect to the field strength. It is therefore appropriate to present a brief review of the various magnetic-field regimes. This part follows closely the discussion in Ref. 2. In the presence of a magnetic field one needs to distinguish between the length scales L, l , the magnetic length $l_H = (eH)^{-1/2}$, and the cyclotron radius $l_c = l_H (E_F / \omega_c)^{-1/2} \sim p_F l_H^2$. Here the cyclotron frequency is $\omega_c \equiv eH/m$. The cyclotron radius may be thought of as the magnetic length of electrons at the Fermi energy.

Depending on the relative magnitude of the magnetic length we group the various regimes into three different classes as follows.

(i) The *weak-field* regimes defined by $l_H > L$, i.e., there is less than one flux quantum enclosed in the system. For diffusive systems this range of the magnetic field splits into two subregimes: The *superweak-field* regime $l_H > (E_c / \Delta)^{1/4} L$ [regime *A* in the notation of Ref. 2(a)]. In the presence of inelastic broadening $\gamma > \Delta$, the rhs of this inequality is replaced by $(E_c / \gamma)^{1/4} L$. We note that for mesoscopic systems, $E_c / \gamma > 1$. The *weak-field* regime (*B*) is defined by $(E_c / \Delta)^{1/4} L > l_H > L$. No similar subclassification has been proposed for ballistic systems.

(ii) The *intermediate-field* regime (*C*), defined by $L > l_H > l$ (for diffusive systems). In Ref. 2(a) this regime was divided into two subregimes. For reasons detailed below, we have concluded that no such division is needed.

(iii) The *strong-field* regimes defined by $l < l_H$ (for diffusive systems). It is divided into subregime *D*, $l_H < l < l_c$, where the field is not yet strong enough to prevent the disorder-induced mixing of adjacent Landau levels. Under this condition, Shubnikov–de Haas oscillations (as well as quantum Hall plateaus) are washed out. Subregime *E* ($l_c < l$, i.e., $\omega_c \tau > 1$) is the quantum Hall regime. This also implies that Shubnikov–de Haas oscillations may be observed. To detect the quantization of the Hall conductance, one usually employs a field stronger than one needed to satisfy $\omega_c \tau > 1$, such that the number of occupied Landau levels is small.

Spectral correlations in the presence of a magnetic field are of interest since the latter represents a source of symmetry breaking. Evidently, one is interested in universal properties of the level statistics and those are mainly affected by changes in symmetries. The field-dependent part of the associated correlation functions is directly related to experimentally measurable quantities.^{21–24} As an example, we refer to the observation that the ensemble-averaged electronic properties of mesoscopic systems (in the presence of some external magnetic field) depend crucially on the type of the employed statistical ensemble. On the one hand, one may vary the applied field adiabatically, keeping the chemical potential (but not necessarily the particle number) of each member of the ensemble fixed. This procedure is usually referred to as *grand canonical*. Alternatively, one may decouple the

system (i.e., each member of the ensemble) from the particle reservoir, thereby keeping the particle number (again of each ensemble member) field independent. This is referred to as a *canonical* procedure. In fact a larger variety of averaging procedures may be defined. Relations between canonical and grand canonical thermodynamic derivatives have been found. The respective magnetizations, for instance, are related to each other through^{1,2,5}

$$\langle M_c \rangle = \langle M_{gc} \rangle - \frac{\Delta}{2} \partial_H \langle \delta N^2 \rangle_\mu, \quad (58)$$

where $\langle \delta N^2 \rangle_\mu \equiv \Sigma_2(\Delta E = \mu; H)$. Evidently, it is the magnetic-field-dependent part of this quantity which counts. Similar relations may easily be derived for higher-order derivatives (e.g., the magnetic susceptibility), as well as for derivatives with respect to other fields (e.g., with respect to an Aharonov-Bohm flux, yielding the persistent current in multiply connected geometries). Level correlations enter in the calculation of mesoscopic *fluctuations*, e.g., fluctuations of the orbital susceptibility too. A detailed discussion of the canonical magnetization as well as its derivation for a variety of field strengths can be found in Ref. 2.

Considerable work has been done on spectral correlations in the presence of a magnetic field. This includes extensive analyses of the GOE-to-GUE transition within random-matrix theory, cf. Ref. 20. For diffusive systems the study of flux-dependent correlations has been extended beyond the random-matrix regime. There are major differences between the effect of an Aharonov-Bohm flux and the effect of a uniform magnetic field.^{2,3} Let us consider the energy scale E_H marking the crossover between small energy scales, over which correlation functions are affected by the field (or flux) due to a broken time-reversal symmetry, and large energy scales, over which spectral correlations are essentially field independent. For diffusive systems $E_H \simeq D/l_H^2$. When considering an Aharonov-Bohm flux, the effective magnetic length always satisfies $l_H > L$: Owing to the flux periodicity the effective flux does not exceed a flux quantum, meaning that in such systems we are always in the weak-field regime. Next, we note that when calculating the *flux-dependent* fluctuations in the number of levels Σ_2 , one needs to integrate the correlation function K over the entire energy range $-E_F < E < E_F$. It turns out, however, that the flux-dependent part of $K(E; H)$ decays exponentially for $E > E_H$. Therefore, only a relatively small energy window will contribute to the flux-dependent part of Σ_2 . Since for Aharonov-Bohm geometries $E_H < E_c$, the flux-dependent contributions to Σ_2 may indeed be calculated within the framework of random-matrix theory (which is applicable for energies smaller than E_c). It turns out that the field-dependent part of Σ_2 is of order unity.

We next review certain points vis-à-vis a uniform applied field that hitherto have been left open.

(a) For a weak magnetic field one may expect a behavior that qualitatively resembles the one discussed in

connection with Aharonov-Bohm geometries. When calculating Σ_2 , it has previously been *assumed*^{1,2,5,13} that field-dependent contributions arise mainly from energy windows smaller than E_c (and in any case not larger than $1/\tau$), yielding field-dependent particle fluctuations that do not exceed an order of unity. That led to a prediction of an anomalously large paramagnetic orbital susceptibility in canonical systems, similar to the prediction of large paramagnetic persistent currents in Aharonov-Bohm geometries. Central to this discussion was the question whether indeed the field dependence of K may be neglected for $\omega > E_c$, or, more quantitatively, how fast does the field-dependent part of $K(\omega)$ decay with ω .

This issue turned up in the analysis of linear-susceptibility fluctuations.^{3,25-28} Such calculations lead to energy integrals over expressions involving field derivatives of spectral correlation functions. Assuming that the dominant contribution to the field-sensitive part of the function K is due to the so-called zero mode (referred to above as the $q=0$ mode), Serota and Oh²⁸ were led to ultraviolet diverging expressions. To obtain finite results, they employed the scale E_c (which limits the range of applicability of the zero-mode approximation) as an upper cutoff. In this way they arrived at

$$\langle \delta \chi^2 \rangle \sim \chi_L^2 (E_F \tau)^2 \ln \left[\frac{E_c}{T^*} \right], \quad (59)$$

i.e., at an expression exhibiting a logarithmic cutoff dependence. Hence χ_L is the Landau susceptibility and

$$T^* \equiv \max\{T, (2\pi\tau_H)^{-1}\},$$

with $\tau_H^{-1} = 2\pi^2 E_c (2\Phi/\Phi_0)^2$. The semiclassical analysis presented below supports the view that E_c is not a natural upper cutoff for the relevant integrals and that the zero-mode approximation is incapable of describing the proper ultraviolet behavior of the integrands. This would imply that Eq. (59) is not correct. Unfortunately, our approach is restricted to energies $\omega > E_c$, which means that we are unable to suggest an alternative result.

(b) A recent analysis of the field-dependent part of Σ_2 revealed the existence of a previously unaccounted for contribution to the orbital magnetization in the diffusive regime. These results were based on the assumption that the low-energy ($\omega < 1/\tau$) correlation functions can be derived within the standard diffusion approximation (which employs diffusons and cooperons), while the contribution of high energies ($\omega > 1/\tau$) is inessential. Below we support the latter assumption by showing that the field-dependent part of $K(\omega, H)$ indeed decays exponentially for sufficiently large energies. On the other hand, we obtain the surprising result that the first assumption has to be abandoned, which implies that some of the findings of Ref. 2(a) need to be revised.

(c) The strong field behavior of Σ_2 has not been discussed previously. We address this field regime and comment on the importance of the field-dependent part of Σ_2 in connection with thermodynamic observables.

We begin our analysis by outlining the diagonalization of the field-dependent ζ , analogous to the discussion of

the field-free case in Sec. II. We consider a two-dimensional sample subject to a perpendicular magnetic field. For $l_c > l$ (i.e., in regimes *A*, *B*, *C*, and *D*), it is possible to show that the magnetic-field-dependent single-particle Green function $G(\omega, H)$ is related to the field-free Green function $G^0(\omega)$ via

$$G(\omega, H; r_1, r_2) = e^{ie \int_{r_1}^{r_2} dr \cdot A} G^0(\omega; r_1, r_2), \quad (60)$$

where the integral is taken along a straight line. The absorption of the magnetic field in a phase factor is commonly referred to as the Bethe-Peierls approximation. Employing the latter and the definition of diffusion and cooperon ξ [Eq. (10)], we are led to

$$\xi^{(C,D)}(\omega, H_{+, -}; r_1, r_2) = e^{ie \int_{r_1}^{r_2} dr \cdot A_{+, -}} \xi^0(\omega; r_1 - r_2),$$

where $H_{\pm} = H_1 \pm H_2$, $H_{\pm} = \nabla \times A_{\pm}$, and ξ^0 is the field-free ξ . The eigenvalue equation for $\xi^{(C,D)}$ reads

$$\xi^{(C,D)} \psi_n^{(C,D)} = \lambda_n^{(C,D)} \psi_n^{(C,D)}, \quad (61)$$

i.e.,

$$\int d^2 r_2 \xi^{(C,D)}(\omega, H_{+, -}; r_1, r_2) \psi_n^{(C,D)}(\omega, H_{+, -}; r_2) = \lambda_n^{(C,D)}(\omega, H_{+, -}) \psi_n^{(C,D)}(\omega, H_{+, -}; r_1). \quad (62)$$

Evidently $\xi^{(C)}$ and $\xi^{(D)}$ differ from each other in the presence of a field. In many instances we are interested in $H_1 \simeq H_2$, which implies that the diffusion contribution may be discussed in the context of the weak-field regime. For reasons that will become clear below, the exact analysis of the eigenvalues turns out to be cumbersome in that limit. One may, however, treat the field dependence as a second-order perturbation correction to the field-free eigenvalues and write

$$\lambda_n^{(C)}(\omega, H) = (-)^n 2\pi \left\{ 2 \left[\frac{l_H}{L} \right]^2 \xi^0(q=0, \omega) + \frac{1}{2\pi} \int_{(2\pi l_H/L)^2}^{\infty} dx e^{-x} L_n(2x) \xi^0(x^{1/2}/l_H, \omega) \right\}, \quad n=0, \dots, \quad (66)$$

where L_n is the Laguerre polynomial of order n . Restricting ourselves to the consideration of the large-field regimes *C* and *D*, we now apply these results to investigate the so-called canonical magnetization. While regime *D* is nondiffusive in the sense of our earlier discussion and has not been analyzed before, regime *C* fulfills all formal requirements to be described in terms of the standard cooperon approximation. Most surprisingly, however, the results of our more general calculation differ substantially from the findings of Ref. 2(a).

Formally, the canonical magnetization resembles the magnetization of dirty superconductors close to the transition point, i.e., apart from a few straightforward manipulations, the calculation presented below amounts to a repetition of a similar calculation contained in the paper of

$$\lambda^{(D)}(q, \omega, H_-) \simeq 1 - i\omega\tau + D\tau q^2 - \alpha \frac{S^2}{l_H^4}, \quad (63)$$

where S is the systems area and α is a geometry-dependent factor.

We now turn our attention to the cooperon contribution. Formally, our analysis follows the lines of Ref. 29, where an eigenvalue equation like Eq. (61) was encountered in the context of dirty superconductors near the transition point. Recalling the Bethe-Peierls approximation, the rhs of Eq. (62) becomes

$$\int d^2 r_2 e^{ie \int_{r_1}^{r_2} dr \cdot A} + \frac{1}{L^2} \times \sum_q e^{iq \cdot (r_1 - r_2)} \xi^0(q, \omega) \psi_n^{(C)}(r_2; \omega, H_+). \quad (64)$$

The evaluation of a very similar expression is detailed in Ref. 30 and we shall not repeat it here. Let us mention, however, that one essential step in the analysis of Lee and Payne was the introduction of polar coordinates for the r_2 integration. In principle, the polar integration is hindered by the presence of system boundaries. Due to the presence of exponential suppression factors $\sim \exp[-(r_2/l_H)^2]$, however, their effect becomes inessential once one demands

$$\left[\frac{L}{l_H} \right]^2 \gg 1. \quad (65)$$

If this relation does not hold, the analysis of Eq. (61) becomes significantly more involved, and the eigenvalues begin to depend on the system geometry, similar to the sample-shape dependence of α in Eq. (63). After some algebra we obtain for regimes *C* and *D* (where both the inequality Eq. (65) and the Bethe-Peierls approximation hold),

Lee and Payne²⁹ on superconductor diamagnetism. To begin with, we derive an expression for Σ_2 in terms of the field-dependent eigenvalues $\{\lambda_n\}$. Substituting the appropriate eigenvalues $\lambda_n(\omega)$ in the general expression Eq. (13) and integrating over energies as in Sec. II, we obtain

$$\Sigma_2(\Delta E, H, H) = \text{Re}[F(\Delta E, H) - F(0, H)], \quad (67)$$

where

$$F(\omega, H) = -\frac{1}{2\pi} \left[\frac{L}{l_H} \right]^2 \sum_n \ln[1 - \lambda_n(\omega, H)]. \quad (68)$$

Substituting this expression in Eq. (58), we obtain

$$\langle M \rangle_c = -\frac{\Delta}{2\pi^2} \lim_{\Delta E \rightarrow \infty} \partial_H \operatorname{Re}[F(\Delta E, H) - F(0, H)]. \quad (69)$$

The differentiation with respect to H then leads to

$$\begin{aligned} \partial_H F(\omega, H) = & -\frac{1}{2\pi H} \left[\frac{L}{l_H} \right]^2 \\ & \times \sum_n \sum_{j=0}^{\infty} \frac{1}{j} \lambda_n^{j-1} [\lambda_n + jH \partial_H \lambda_n]. \end{aligned} \quad (70)$$

As will become apparent below, both terms appearing in the square brackets cancel each other to a large extent. For this reason, it is essential to calculate the derivative $H \partial_H \lambda_n$ as accurately as is possible. A more elegant way of performing the differentiation exactly was found by Lee and Payne. Making use of recurrence relations fulfilled by the Laguerre polynomials [cf. the definition of λ_n , Eq. (66)], one obtains as a result of a short calculation of purely algebraic expression

$$H \partial_H \lambda_n = \frac{n+1}{2} (\lambda_{n+1} - \lambda_n) + \frac{n}{2} (\lambda_n - \lambda_{n-1}). \quad (71)$$

Insertion of this result in Eq. (70) leads to

$$\begin{aligned} \partial_H F(\omega, H) \frac{1}{2\pi H} \left[\frac{L}{l_H} \right]^2 \sum_n \left\{ \ln(1 - \lambda_n) \right. \\ \left. - \frac{(n+1)(\lambda_{n+1} - \lambda_n) + n(\lambda_n - \lambda_{n-1})}{2(1 - \lambda_n)} \right\}. \end{aligned} \quad (72)$$

Note that contributions of order λ_n and λ_n^2 corresponding to diagrams S_1 and S_2 exactly cancel each other. This is an (admittedly rather intricate) proof of the physically obvious fact that these diagrams are field independent in Bethe-Peierls approximation. A closed trajectory, involving only one or two impurity scattering events (and no boundary scattering) cannot enclose the magnetic flux.

Instead of evaluating both the summation Eq. (72) and the eigenvalue integration Eq. (66) numerically, one may tentatively resort to some approximations. At least in regime C and for $n < (l/l_H)^{-2}$ the factor $x(l/l_H)^2$ appearing in the integrand of Eq. (66) is smaller than unity and one may expand according to

$$\begin{aligned} \lambda_n(\omega, H) &= (-)^n \int_0^{\infty} dx e^{-x} L_n(2x) \frac{1}{[(1-i\omega\tau)^2 + 1/2x(l/l_H)^2]^{1/2}} \\ &\simeq (-)^n \int_0^{\infty} dx e^{-x} L_n(2x) \left[1 + i\omega\tau - \frac{x}{4} \left[\frac{l}{l_H} \right]^2 \right] \\ &= 1 + i\omega\tau - (n + \frac{1}{2}) \left[\frac{l}{l_H} \right]^2. \end{aligned} \quad (73)$$

Since this form of the eigenvalues leads immediately to the standard cooperon, we will refer to Eq. (73) as the diffusive approximation. With this expression for λ_n , the sum Eq. (72) can be calculated analytically and we rediscover the result of Ref. 2(a), i.e., a constant magnetization

$$\langle m_c \rangle_c^{\text{diff}} = \frac{\ln 2 e \Delta L^2}{16 m a \pi^3}. \quad (74)$$

For values $(l/l_H)^2 \ll 1$, the necessary restriction of the sum to values $n < (l/l_H)^{-2}$ is of minor importance. This can be read off from Fig. 7, where we have plotted the properly restricted sum (dash-dotted line) together with the unrestricted sum (broken line) as a function of the magnetic field [cf. also the discussion in Ref. 2(a)]. As soon as we approach regime D , i.e., the ratio l/l_H approaches unity, the diffusion approximation breaks down, and the integration Eq. (66) can no longer be carried out exactly. Within an accuracy of 0.15% (3%) for

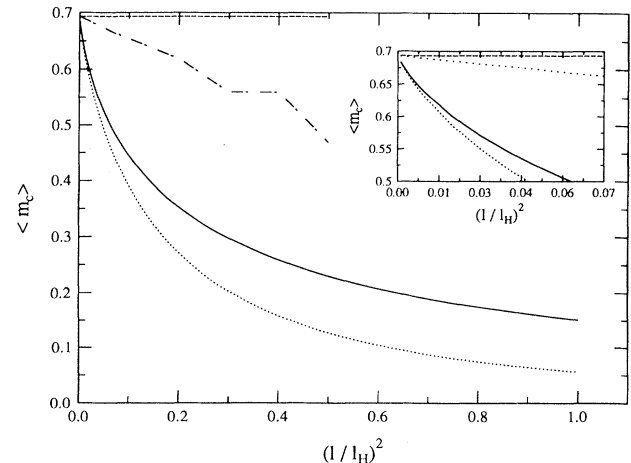


FIG. 7. Canonical magnetization plotted vs magnetic-field strength. For an explanation, see the text.

$(l/l_H)^2=0.1$ [$(l/l_H)^2=1$], however, the result may be approximated according to

$$\lambda_n(\omega, H) = (-)^n \int_0^\infty dx e^{-x} L_n(2x) \times \frac{1}{[(1-i\omega\tau)^2 + (x/2)(l/l_H)^2]^{1/2}} \simeq \frac{1}{[(1-i\omega\tau)^2 + 2(n + \frac{1}{2})(l/l_H)^2]^{1/2}}. \quad (75)$$

Substitution of this form in Eq. (72) and summation over n (numerically) leads to a magnetization that is shown as a solid line in Fig. 7. In order to check the validity of the approximation, we have computed both integration over the Laguerre polynomials as well as the subsequent n summation numerically. The result (dotted line in Fig. 7) agrees qualitatively with the one based on Eq. (75).

Most surprisingly, exact and diffusive forms of λ_n , respectively, lead to remarkably different results *even in regime C*. Notwithstanding the results of Ref. 2(a), we obtain a nonconstant, monotonously decreasing magnetization, which could hardly be interpreted in terms of corrections to an essentially constant magnetization (cf. Fig. 7). From the technical point of view, this result is somewhat disturbing since it demonstrates the invalidity of the approximation Eq. (73) in a regime where it is commonly adopted.

It should also be noted that a further subdivision of the intermediate field regime as in Ref. 2(a) is not necessary. It has been postulated there that the low-lying cooperon eigenstates contribute differently once their spatial extension becomes comparable with L . But this is not quite so. As long as the Bethe-Peierls approximation holds, the eigenstates are determined by the integral equation (61). The field-free Green functions extend over an area of order l^2 . Thus, in most cases [i.e., apart from corrections of order $(l/L)^2$] the integration will not be sensitive to boundary effects, which implies that a division into two subregimes is superfluous.

The above analysis applies to regime *D* as well. It turns out that the field-dependent contributions to Σ_2 are so strongly suppressed that the canonical contribution to the magnetization is not relevant in these regimes, i.e., it is significantly exceeded by the Landau diamagnetic term.

We have stressed earlier that our approach holds for ballistic systems as well. We have obtained some indications that an interesting field-dependent behavior is expected for this range of disorder (including cases of enhanced field sensitivity as compared with diffusive systems). A full scale analysis of the ballistic case, however, is significantly more intricate than the one presented here and has not yet been completed.³⁰

The analysis of spectral correlations in the weak-field regimes is seriously hindered when $l_H > L$. The approximation based on the inequality Eq. (65) cannot be taken. One may yet try to solve the eigenvalue problem Eq. (61). As an alternative we present in Appendix C a totally different approach based on a semiclassical analysis of the two-level correlation function. Parts of the discussion but not the conclusions concerning the effects on K and Σ_2 have been addressed in Ref. 8. As a result we obtain

$$K(\omega) \xrightarrow{\omega > E_c} \text{const} \times \cosh^{-2} \left[\frac{\pi\omega\Phi_0}{2E_c\Phi} \right] + R, \quad (76)$$

where R denotes the field-independent contribution to the correlation function that has been discussed earlier and is not of interest here. In a strict sense, this form is justified only for $\omega > E_c$. Equation (76) confirms the prevailing belief that there are indeed no significant contributions to field-dependent thermodynamic quantities from energies larger than the magnetic energy $E_H = E_c \Phi / \Phi_0$. Equation (76) suggests that for $\Phi < \Phi_0$ the upper energy scale limiting the range of magnetic-field sensitivity is parametrically smaller than E_c . For energies larger than E_c , the field sensitivity is exponentially small. As mentioned above, this behavior is incompatible with the logarithmic E_c dependence predicted by Eq. (59).

VI. CONCLUDING REMARKS

The discussion presented here consists conceptually of two parts. In the first one we develop a formalism that enables us to calculate the disorder-averaged two-level correlators and subsequently the level number fluctuations Σ_2 . Our analysis underlines the existence of a ballistic regime $L < l$, which cannot be described within the framework of clean systems. Our study also stresses the importance of correlations over large energy intervals, which so far have been largely ignored (or have been treated heuristically). Most parts of our analysis have semiclassical counterparts, and therefore a semiclassical treatment of this problem (parts of which have already been published) is called for.

The second conceptual part of our analysis is the introduction of various averaging schemes. The fact that one may average over energy, disorder, and system sizes allows for the definition of several differently averaged correlation functions. We have chosen to discuss only two, which to us seem most practical. These correlation functions provide a crossover from predominantly energy-averaged functions (where spatial disorder plays no important role, e.g., in clean chaotic systems) to predominantly impurity-averaged functions (pertinent in mesoscopic physics). A typical ensemble of electronic systems (e.g., an ensemble of quantum dots) is characterized by sample-to-sample size fluctuations, which are large in comparison with the Fermi wavelength. A realistic description of the ensemble average should thus include a simultaneous average over both disorder and sizes. We have shown that the sample-size averaging may drastically affect the spectral statistics of ballistic ensembles. On the other hand, one may consider an experiment on a macroscopic microwave cavity, where the confining potential may be varied in a controlled way. For that type of experiment one should not employ size averaging. In conclusion, we believe that the various averaging procedures proposed here may, in principle, be put to a test.

These are some obvious extensions and generalizations of the present analysis. One may apply the same methods to higher-dimensional systems. Other types of disorder correlations may also be studied. But perhaps the most

promising direction is to address the question of magnetic-field correlations in ballistic systems. As has been mentioned above, we have some preliminary indications that these correlations may be of significant magnitude.

ACKNOWLEDGMENTS

We have benefited from discussions with N. Argaman, Y. Imry, A. Kamenev, Y. Levinson, B. Shapiro, U. Smilansky, and H. A. Weidenmüller. A.A. acknowledges MINERVA for financial support. This work was supported by the German-Israel Foundation (GIF) and the U.S.–Israel Binational Science Foundation (BSF).

APPENDIX A: DIAGONALIZATION OF THE OPERATORS ζ

This appendix is devoted to an approximate diagonalization of the integral operator ζ , which is a solution of the integral equation (16) up to corrections in the disorder parameter $p_F l$. We consider the model system introduced in Sec. II, i.e., the Green functions entering Eq. (16) are those defined in Eq. (15) and no distinction between $\zeta^{(d)}$ and $\zeta^{(c)}$ is required.

As long as the sample is diffusive, $L \gg l$, Eq. (16) possesses a set of slowly varying solutions

$$\begin{aligned} \psi_q(r) &= \prod_{i=1,2} a_{q_i} \cos(q_i r_i), \\ a_{q_i} &= \begin{cases} L^{-1/2}, & q_i = 0 \\ L^{-1/2} \sqrt{2}, & q_i \neq 0, \end{cases} \quad q_i = \frac{n_i \pi}{L}, \quad n_i = 0, 1, \dots \end{aligned} \quad (\text{A1})$$

with $ql \ll 1$ and eigenvalues

$$\lambda(q, \omega) = 1 - i\omega\tau + D\tau q^2, \quad (\text{A2})$$

where D is the diffusion constant. To the best of our knowledge, all concrete derivations showing that the modes Eq. (A1) solve Eq. (16) (cf., e.g., Ref. 14) rely on their slow variation on scales of the mean free path, a restriction that has to be abandoned in the nondiffusive regimes. Still, there exists a general physical argument in favor of cosine functions as promising candidates for eigenfunctions that is independent of the oscillation rate. The point is that ζ is directly related to the density-density response kernel, i.e., its normal derivative taken at the boundary is a measure for the current leaving the system. In the case under consideration, this implies that eigenfunctions of ζ have to fulfill Neumann boundary conditions. In the following, we argue that the functions Eq. (A1) indeed solve the integral equation within the desired accuracy, even if the condition of slow variation is abandoned. Substituting Eqs. (A1) and (15) in Eq. (16) and performing the coordinate integrations, we arrive at

$$\begin{aligned} & \frac{1}{L^2} \prod_{i=1,2} \sum_{p_i} \{ \sin^2(p_i r_i) \cos(q_i r_i) \\ & + 2 \sin(2p_i r_i) \sin(q_i r_i) \} D^+(\epsilon_1, p) D^-(\epsilon_2, p+q) \\ & = \lambda(q, \omega) \prod_{i=1,2} \cos(q_i r_i), \end{aligned} \quad (\text{A3})$$

where \sum_{p_i} denotes the summation over positive and negative modes $p_i = 0, \pm\pi L^{-1}, \pm 2\pi L^{-1}, \dots$. As for the p -dependent trigonometric functions appearing in the curly brackets, the p summation effectively amounts to an average over the Fermi surface. The reason is that the energy denominators D^\pm are strongly peaked at $p = O(p_F)$ but depend only weakly on the direction of p , while for typical values $r_i = O(L)$ the sine and cosine functions oscillate with period $O(p_F/L)$. In the case $ql \gg 1$ not the whole Fermi circle but only two angular sections of width $2\pi/(ql)^{1/2}$ contribute significantly to the p sum. In this region, however, the energy denominators are still smooth functions of p and the subsequent argument remains applicable. We now argue that each contribution to the Fermi-surface-averaged product of trigonometric functions involving a factor $\sin(2p_i r_i)$, $i=1,2$ is small in the sense of the $p_F l$ expansion. The point is that $\sin^2(p_i r_i)$ is a positive-definite function with mean value $\frac{1}{2}$ while $\sin(2p_i r_i)$ rapidly changes sign. This consideration can be made quantitative by exploiting that variations of the arguments r_i on atomic scales are inessential for our purpose. Upon averaging the coordinates r in Eq. (A3) with a Gaussian weight $\sim \exp[-(r_i + \delta r)^2/a^2]$, where a is large in comparison with the atomic distance $O(p_f^{-1})$ but small in comparison with any other length scale in the problem, terms involving a function $\sin(q_i r_i)$ acquire a suppression factor $\sim \exp[-(p_i a)^2] = O(\exp[-(p_f a)^2]) \ll 1$, while pure cosine terms remain unaffected. One might object that not only $p_i = O(p_f)$ but also small momentum components p_i , to which the argument cannot be applied, contribute to the p summation. For example, one has a region on the p_f shell where $p_1 \simeq p_f$ and p_2 is small, rendering the r_2 coarsening of $\sin(2p_2 r_2)$ ineffective. This objection can be refuted by performing the Fermi-surface summation over p before applying the procedure outlined above. Upon retaining only the first terms in the curly brackets and approximating $\langle \prod_{i=1,2} \sin^2(p_i r_i) \rangle_{\text{Fermi surf}} \simeq \frac{1}{4}$, we find the eigenvalue equation to be solved with eigenvalues

$$\lambda(q, \omega) = \frac{1}{8\pi\nu\tau L^2} \sum_{p_i} D^+(\epsilon_1, p) D^-(\epsilon_2, p+q). \quad (\text{A4})$$

The evaluation of the sum Eq. (A4) is simplest in the diffusive case. For $l \ll L$, the disorder-induced broadening of the Fermi circle in p space ($\sim l^{-1}$) exceeds the spacing between the p modes ($\sim L^{-1}$), hence the sum may be replaced by an integral. As a result of the integration one obtains Eq. (18). In the ballistic case, however, the disorder does not suffice to smear the structure of the individual modes and the sum has to be retained. Application of the Poisson sum rule (cf. Sec. IV) leads to

$$\begin{aligned} \lambda(q, \omega) &= \frac{1}{8\pi\nu\tau} \sum_{k \in \mathbb{Z}^2} \int p dp \int_0^{2\pi} d\theta e^{ipL_k \cos\theta} D^+(\epsilon_1, p) \\ & \quad \times D^-(\epsilon_2, p+q), \end{aligned} \quad (\text{A5})$$

where $\sum_{k \in \mathbb{Z}^2}$ is an abbreviation for the summation over all pairs $k = (k_x, k_y)$, $k_i = 0, \pm 1, \dots$, $L_k^T = 2L(k_x, k_y)$,

$L_k = |\mathbf{L}_k|$, and $\theta = \angle(\mathbf{p}, \mathbf{L}_k)$. We evaluate Eq. (A5) separately for energies larger and, respectively, smaller than the inverse time of flight $t_f = L/v_f$. In the latter case, the contribution of nonzero modes $\lambda(q \neq 0, \omega)$ to the correlation functions is negligible (cf. the text). Performing the pole integration over p we arrive at

$$\lambda(0, \omega) = \frac{1}{8\pi\nu\tau} \sum_{k \in \mathbb{Z}^2} \int_0^{2\pi} d\theta \exp \left[ip_F L_k \cos\theta - \frac{L_k}{l} |\cos\theta| \right] \times \frac{m\tau}{1+i\omega\tau} + O(\omega t_f). \quad (\text{A6})$$

At this point it is essential to remember that the density

of states is also to be calculated as a discrete sum, i.e.,

$$\nu = \frac{1}{4\pi L^2} \text{Im} \sum_p G^+(p, 0) = m \sum_{k \in \mathbb{Z}^2} \int_0^{2\pi} d\theta \exp \left[ip_F L_k \cos\theta - \frac{L_k}{l} |\cos\theta| \right]. \quad (\text{A7})$$

Inserting this expression in Eq. (A6) we obtain $\lambda(0, \omega) = (1+i\omega\tau)^{-1}$, i.e., the same expression as in the diffusive case. As soon as we approach $\omega \sim t_f^{-1}$, higher modes $\lambda(q \neq 0, \omega)$ have to be taken into account. Performing the pole integration over p we obtain instead of Eq. (A6),

$$\lambda(0, \omega) = \frac{1}{8\pi\nu\tau} \sum_{k \in \mathbb{Z}^2} \int_0^{2\pi} d\theta \exp \left[ip(q, \omega) L_k \cos\theta - \frac{L_k}{l} |\cos\theta| \right] \frac{m\tau}{1+i\omega\tau + iql \cos\theta}, \quad (\text{A8})$$

where $p(q, \omega)$ denotes the pole value whose dependence on ω and q must no longer be neglected and $\tilde{\theta}$ is the angle enclosed by q and p . Due to the entanglement of the vectors q , p , and L_k , the result of the θ integration will in general depend on the Fermi energy and the orientation of the mode vector q with respect to the boundary. As a consequence of the rapid oscillation of the θ -dependent phase factor, however, the dominant contribution to the integral comes from $\theta \sim 0$ as long as $L_k \neq 0$. Linearization of $\cos(\theta)$ around $\theta = 0$ shows that $L_k \neq 0$ contributions to the sum are of order $\cos(p_F L_k) \exp(-L_k/l)(p_F L_k)^{1/2}$ after the integration. Suffering from both a rapid phase dependence and a factor $O(p_F L)^{-1/2} \ll 1$, these terms will henceforth be regarded as negligible. Apart from a weak energy dependence of the parameters τ and l , the product $[\lambda(q, \omega)^0]^n$ is insensitive against energy averaging. The $\lambda(q, \omega)'$, however, depend on the Fermi energy via the large phase $p_F L_k \cos(\theta) = O(p_F L \cos(\theta))$. From the discussion of Sec. III, it is clear that a factor $[\lambda(q, \omega)']^n$ will average to a term of order $\exp(-E_0 t_f) \ll 1$ if n is odd and $(p_F l)(-n/2) \ll 1$ if n is even. We therefore have $\langle \lambda(q, \omega)^n \rangle_{E_0} \simeq \langle [\lambda(q, \omega)^0]^n \rangle_{E_0}$. On the other hand, we would have obtained $[\lambda(q, \omega)^0]^n$ immediately, had we approximated the sum over p by an integral from the outset. In other words, averaging the correlation function over energies larger than the inverse time of flight renders the discreteness of the levels inessential. Similarly to averaging over the Fermi energy, the phase-dependent terms can also be discarded by allowing for sample-to-sample fluctuations in the system size with $\delta L p_F \gg 1$.

To summarize, we may take Eq. (A4) as eigenvalues and Eq. (A1) as eigenmodes for all relevant values of the parameters $\omega\tau$ and lq .

APPENDIX B: SINGLE-IMPURITY SCATTERING

In this appendix we study the contribution of the single-impurity scattering process S_1 to the correlation functions. Diagrammatically, S_1 can be represented as

$$S_1 = \left(\text{Diagram} \right), \quad (\text{B1})$$

where the location x of the impurity is integrated over. In an infinite system translational invariance prevents any momentum flow through the impurity line. In this case the diagram S_1 is readily expressed as a decoupled product of two momentum integrations over Green functions and vanishes. Within the semiclassical interpretation this means that in an infinite system at least two impurity scattering events are required to form a closed phase-space trajectory. In this aspect ballistic samples behave differently, since not only impurities but also the boundaries may serve as scattering centers. To study the effect of boundary scattering we substitute the hard-wall Green function Eq. (15) in Eq. (B1) and integrate over x . As a result of a straightforward calculation we get

$$S_1 = \frac{1}{4} \partial_{\epsilon_1, \epsilon_2}^2 \text{Re} \frac{1}{1+i(\epsilon_1 - \epsilon_2)\tau}. \quad (\text{B2})$$

In contradistinction to the previously considered diagrams S_n , $n \geq 2$, there is no summation over q -momentum modes [cf. Eq. (19)]. The reason is that a system boundary can only flip momentum components, i.e., it does not allow for arbitrary momentum exchange like an s -wave impurity scatter. This leads to a reduction in

degrees of freedom and renders the contribution of S_1 to the correlation functions inessential: For small energies $\omega < 1/\tau$ the behavior of the correlation functions is governed by the diffusion pole and low-order diagrams S_i , $i = O(1)$ are insignificant anyhow. In the large-energy limit $E > 1/\tau$, however, the contribution of S_1 is by far less than that of S_2 [cf. Eq. (40)].

APPENDIX C: SEMICLASSICAL ANALYSIS OF THE FIELD-DEPENDENT PART OF THE CORRELATION FUNCTION

The fact that for diffusive systems $p_F l \gg 1$ implies that between two consecutive scattering events the electron, viewed as a classical particle, propagates along straight lines (unless the field is too strong). Evidently, we need to assign a quantum phase to each semiclassical trajectory, considering probability amplitudes rather than probabilities. For both weak- and intermediate-field regimes, the Bethe-Peierls approximation is valid and the phase associated with a given close path is $2\pi\Phi/\Phi_0$, where $\Phi = SH$ is the flux enclosed by the path. Here, S is the enclosed area. It is assigned a plus or minus sign depending on whether that particular path winds clockwise or anti-clockwise, respectively. Let us first try to estimate the field sensitivity of the return probability in real space. Throughout this section we consider time scales shorter than the diffusion time through the system. We thus exclude energy scales smaller than E_c . Parts of the present discussion, but not the final conclusions concerning the correlation functions, have appeared in Ref. 8.

It has been shown that the probability distribution to find a returning path (in an infinite two-dimensional diffusive system) of length \mathcal{L} , enclosing an algebraic area S is³¹

$$P(S) = \frac{\pi}{2\mathcal{L}l} \left[\cosh \left[\frac{\pi S}{\mathcal{L}l} \right] \right]^{-2}. \quad (C1)$$

$P(S)$ is normalized according to

$$\int_{-\infty}^{\infty} dS P(S) = 1.$$

The total classical probability density to return to the origin at time t is $1/(2\pi Dt)$. Noting that $D = v_f l/2$, $\mathcal{L} = v_f t$,

we write this probability as $1/(\pi l \mathcal{L})$. Thus the classical probability density of a returning path of length \mathcal{L} enclosing an area S is given by

$$P(\mathcal{L}, S) = \frac{1}{2\mathcal{L}^2 l^2} \left[\cos \left[\frac{\pi S}{\mathcal{L}l} \right] \right]^{-2}. \quad (C2)$$

Recalling weak localization theory and accounting for the fact that the following ensemble-averaging contributions to the quantum-mechanical return probability arise only from products of the i th returning path with itself or with the amplitude of the time-reversed path, we thus obtain the quantum-mechanical return probability at time $t = \mathcal{L}/v_f$,

$$\begin{aligned} P_{\text{QM}}(t) &= \frac{1}{2\mathcal{L}^2 l^2} \int_0^\infty dS \left[\cosh \left[\frac{\pi S}{\mathcal{L}l} \right] \right]^{-2} \\ &\quad \times \left[2 + 2 \cos \left[\frac{2SH}{\Phi_0} \right] \right] \\ &= \frac{1}{\pi l \mathcal{L}} \left[1 + \frac{2\mathcal{L}lH/(2\Phi_0)}{\sinh[2\mathcal{L}lH/(2\Phi_0)]} \right]. \end{aligned} \quad (C3)$$

This probability is expressed as an integral over contributions from all returning paths of a given length \mathcal{L} . The interference of a trajectory with its time-reversed counterpart [the second term in the integrand of Eq. (C3), identified as the Cooper-channel contribution] is field sensitive. For $H=0$, Eq. (C3) yields the well-known factor-two enhancement of the return probability. According to the analysis of Ref. 8, the sum over products of semiclassically evaluated transition amplitudes and mutually time-reversed transition amplitudes [Eq. (C3) in our case] has to be multiplied by t and energy Fourier transformed in order to yield the correlation function K . Performing the calculation we arrive at the result Eq. (76). Since we consider here time scales shorter than the diffusion time across the system [the effect of boundaries was ignored in Eq. (C1)], our final result should apply for frequencies $\omega > E_c$.

*Present address: Universität zu Köln, Zùlpicher Strasse 77, 50937 Köln, Germany.

¹Y. Imry, in the *Proceedings of the November 1991 Taniguchi Symposium on Mesoscopic Systems*, edited by H. Fukuyama and T. Ando (Springer, Berlin, 1992).

²(a) B. L. Altshuler, Y. Gefen, Y. Imry, and G. Montambaux, *Phys. Rev. B* **47**, 10335 (1993); (b) Y. Gefen, B. Reulet, and H. Bouchiat, *ibid.* **46**, 15922 (1992).

³S. Oh, A. Yu. Zyuzin, and R. A. Serota, *Phys. Rev. B* **44**, 8858 (1991); R. A. Serota and A. Y. Zyuzin, *ibid.* **47**, 6399 (1992).

⁴H. F. Cheung, E. K. Riedel, and Y. Gefen, *Phys. Rev. Lett.* **62**, 587 (1989).

⁵A. Schmid, *Phys. Rev. Lett.* **66**, 80 (1991); B. L. Altshuler, Y. Gefen, and Y. Imry, *ibid.* **66**, 88 (1991); F. von Oppen and E. K. Riedel, *ibid.* **66**, 84 (1991).

⁶A. Altland, S. Iida, A. Müller-Groeling, and H. A. Weidenmüller, *Europhys. Lett.* **20**, 155 (1992); *Ann. Phys. (N.Y.)* **219**, 148 (1992).

⁷A. Kamenev, Y. Gefen, B. Reulet, and H. Bouchiat, *Europhys. Lett.* **26**, 391 (1994).

⁸N. Argaman, Y. Imry, and U. Smilansky, *Phys. Rev. B* **47**, 4440 (1993).

⁹To be more precise, the relationship between K and the classical return probability requires not only the applicability of

- the semiclassical approximation but also the absence of stable islands in the classical phase space. The latter condition is met due to the presence of *stochastic* disorder (disorder averaging leads to a destruction of any stable phase-space regions that may be present in individual samples).
- ¹⁰In systems exhibiting chaotic boundary scattering, an additional energy scale τ' related to the Lyapunov exponent has to be introduced and one may expect significant spectral correlations up to energy scales $\max(\tau^{-1}, \tau'^{-1})$.
- ¹¹G. Casati, B. V. Chirikov, and I. Guarneri, Phys. Rev. Lett. **54**, 1350 (1985).
- ¹²U. Sivan and Y. Imry, Phys. Rev. B **35**, 6074 (1987).
- ¹³B. L. Al'tshuler and B. I. Shklovskii, Zh. Eksp. Teor. Fiz. **91**, 220 (1986) [Sov. Phys. JETP **64**, 127 (1986)].
- ¹⁴For the diffusive regime, this result has been first obtained by E. Abrahams, P. W. Anderson, and T. V. Ramakrishnan, Philos. Mag. B **42**, 827 (1980).
- ¹⁵K. B. Efetov, Adv. Phys. **32**, 53 (1983).
- ¹⁶The same result for K in the regime $D2$ has recently been obtained by I. V. Lerner (private communication).
- ¹⁷K. B. Efetov and V.N. Prigodin, Phys. Rev. Lett. **70**, 1315 (1993). After this work had been completed we were notified that a similar result has recently been derived by Efetov and Prigodin.
- ¹⁸M. Sieber (private communication).
- ¹⁹M. V. Berry, Proc. R. Soc. London Ser. A **400**, 229 (1985).
- ²⁰N. Dupuis and G. Montambaux, Phys. Rev. B **43**, 14 390 (1991); A. Altland, K. B. Efetov, and S. Iida, J. Phys. A **26**, 3545 (1993).
- ²¹L. P. Levy, G. Dolan, J. Dunsmuir, and H. Bouchiat, Phys. Rev. Lett. **64**, 2074 (1990); L. P. Levy, Physica B **167**, 50 (1990).
- ²²V. Chandrasekhar, R. A. Webb, M. J. Brady, M. B. Ketchen, W. J. Gallagher, and A. Kleinsasser, Phys. Rev. Lett. **67**, 3578 (1991).
- ²³D. Mailly, C. Chapelier, and A. Benoit, Phys. Rev. Lett. **70**, 2020 (1993).
- ²⁴L. P. Levy, D. H. Reich, L. Pfeiffer, and K. West, Physica B **189**, 204 (1993).
- ²⁵O. D. Cheishvili, Pis'ma Zh. Eksp. Teor. Fiz. **48**, 206 (1988) [JETP Lett. **48**, 225 (1988)].
- ²⁶H. Fukuyama, J. Phys. Soc. Jpn. Lett. **58**, 47 (1989).
- ²⁷E. Akkermans and B. Shapiro, Europhys. Lett. **11**, 467 (1990).
- ²⁸R. A. Serota and S. Oh, Phys. Rev. B **41**, 10 523 (1990).
- ²⁹P. A. Lee and M. G. Payne, Phys. Rev. B **5**, 923 (1972).
- ³⁰A. Altland and Y. Gefen (unpublished).
- ³¹See, e.g., B. Duplantier, J. Phys. A **22**, 3033 (1989); W. Zwerger and T. Brandes, Z. Phys. B **87**, 89 (1992), and references therein.